US 20160274020A1

(19) **United States**

(12) **Patent Application Publication**

WINKLER et al.

(10) **Pub. No.: US 2016/0274020 A1**

(43) **Pub. Date: Sep. 22, 2016**

(54) **INTEGRATED AND STANDALONE LABEL AND REAGENT-FREE MICROFLUIDIC DEVICES AND MICROSYSTEMS FOR DIFFERENTIAL WHITE BLOOD CELL COUNTS**

(71) Applicant: **UNIVERSITY OF MARYLAND**, College Park, MD (US)

(72) Inventors: **Thomas E. WINKLER**, Greenbelt, MD (US); **Hadar Shumel BEN-YOAV**, Rockville, MD (US); **Reza GHODSSI**, Potomac, MD (US)

(73) Assignees: **UNIVERSITY OF MARYLAND**, College Park, MD (US); **University of Maryland**, Baltimore, MD (US)

(21) Appl. No.: **15/034,719**

(22) PCT Filed: **Nov. 17, 2014**

(86) PCT No.: **PCT/US2014/065913**

§ 371 (c)(1),
(2) Date: **May 5, 2016**

Related U.S. Application Data

(60) Provisional application No. 61/905,028, filed on Nov. 15, 2013.

Publication Classification

(51) **Int. Cl.**

G01N 15/10	(2006.01)
G01N 15/12	(2006.01)
B01L 3/00	(2006.01)

(52) **U.S. Cl.**

CPC ***G01N 15/1056*** (2013.01); ***B01L 3/502707*** (2013.01); ***B01L 3/502776*** (2013.01); ***B01L 3/502761*** (2013.01); ***G01N 15/1218*** (2013.01); *G01N 2015/1062* (2013.01); *G01N 2015/1006* (2013.01); *G01N 2015/008* (2013.01)

(57) **ABSTRACT**

A method of establishing a differential white blood cell count includes directing at least one stream of deionized water into a microfluidic device containing a sample of whole blood or a cell-rich fraction to generate a lysate stream of intact white blood cells; directing at least one stream of deionized water into the lysate stream to form a virtual non-conductive aperture in a channel of the device; and performing impedance cytometry of the lysate stream via coplanar electrodes to detect the presence of intact white blood cells. A microfluidic device includes a blood separation section. An analyte sensor detects electrical changes in a cell-free fraction. Lysate from a cell-rich fraction is analyzed to detect circulating tumor cells or white blood cells including neutrophils, lymphocytes, monocytes, eosinophils, and basophils. A method of fabricating and a standalone cell-rich microfluidic device are disclosed for differential white blood cell counts.

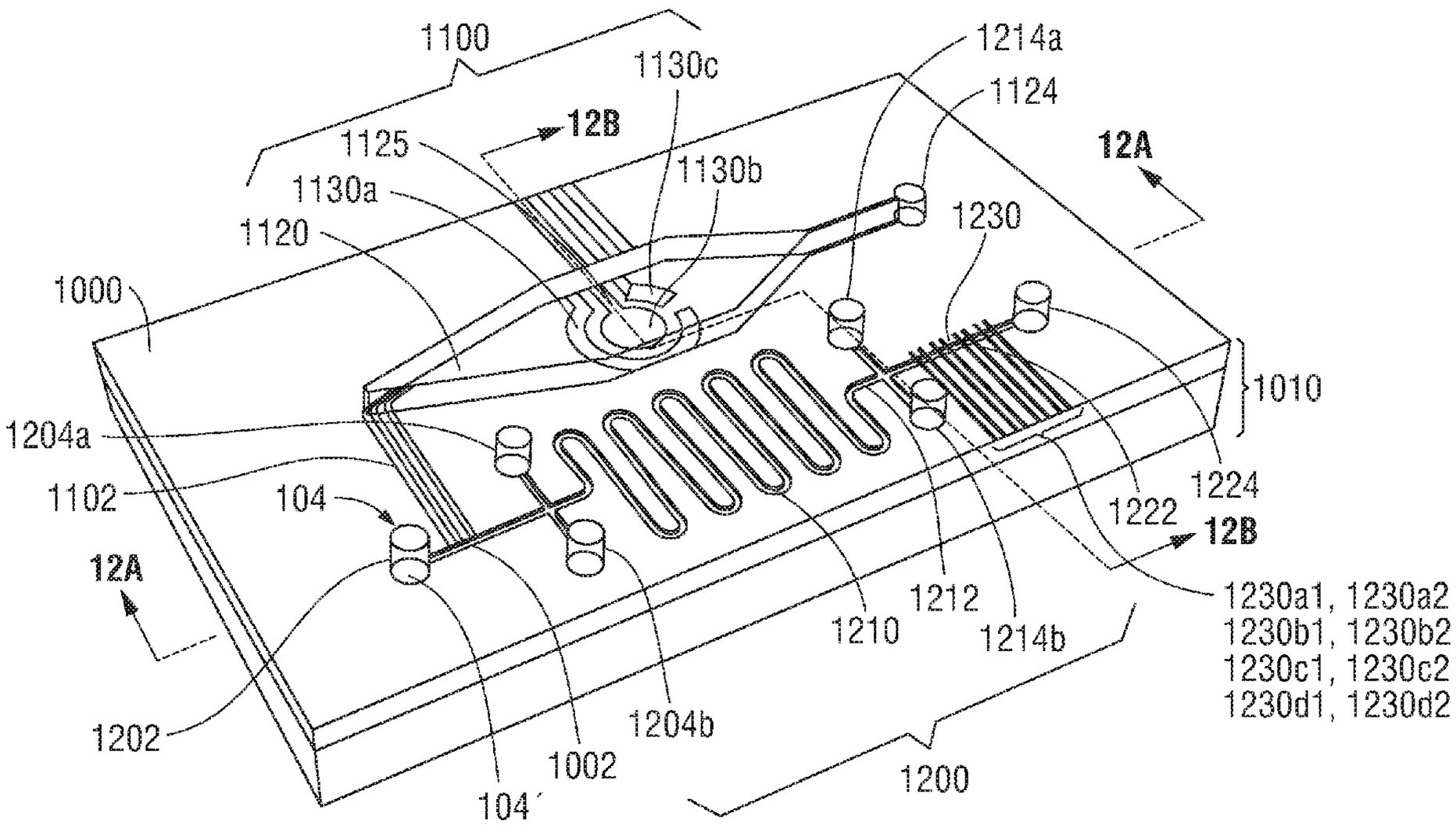

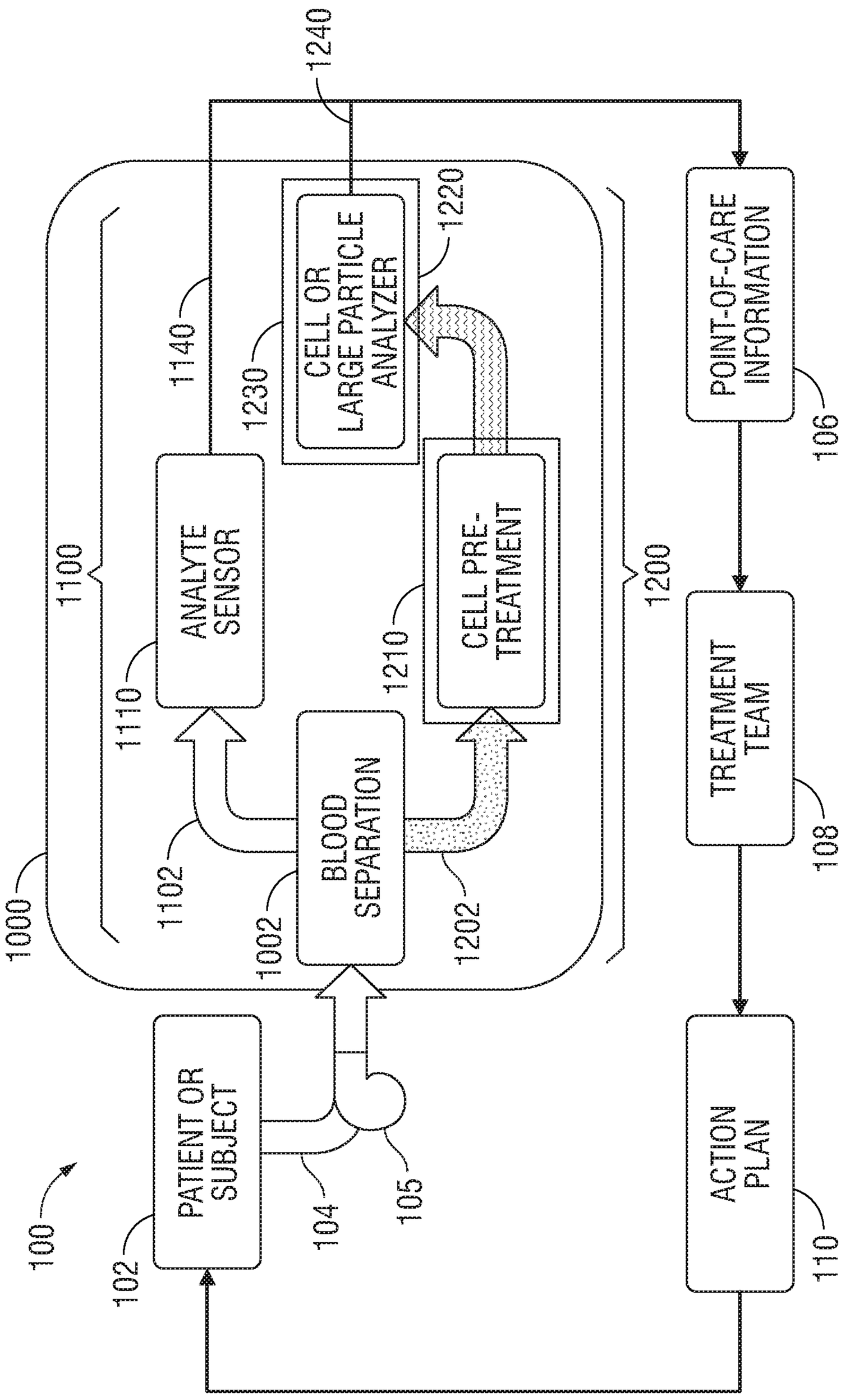
100
102
PATIENT OR SUBJECT
104
105
106
108
110
1000
1002
1100
1102
1110
1140
1200
1202
1210
1220
1230
1240
BLOOD SEPARATION
ANALYTE SENSOR
CELL OR LARGE PARTICLE ANALYZER
CELL PRE-TREATMENT
POINT-OF-CARE INFORMATION
TREATMENT TEAM
ACTION PLAN

FIG. 1

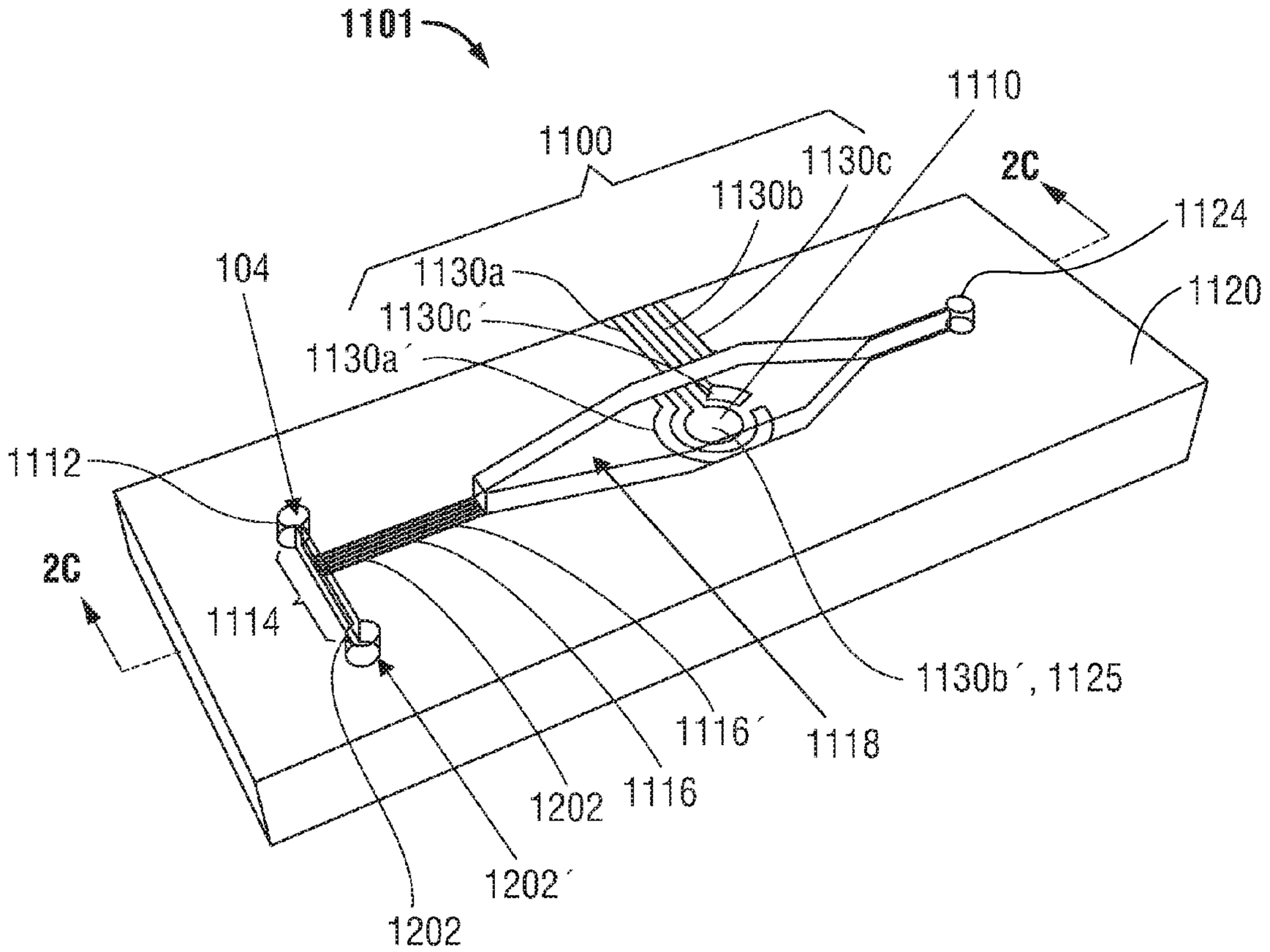
1101
1110
1100
1130c
1130b
2C
1124
104
1130a
1120
1130c´
1130a´
1112
2C
1114
1130b´, 1125
1116´
1118
1202
1116
1202´
1202

FIG. 2A

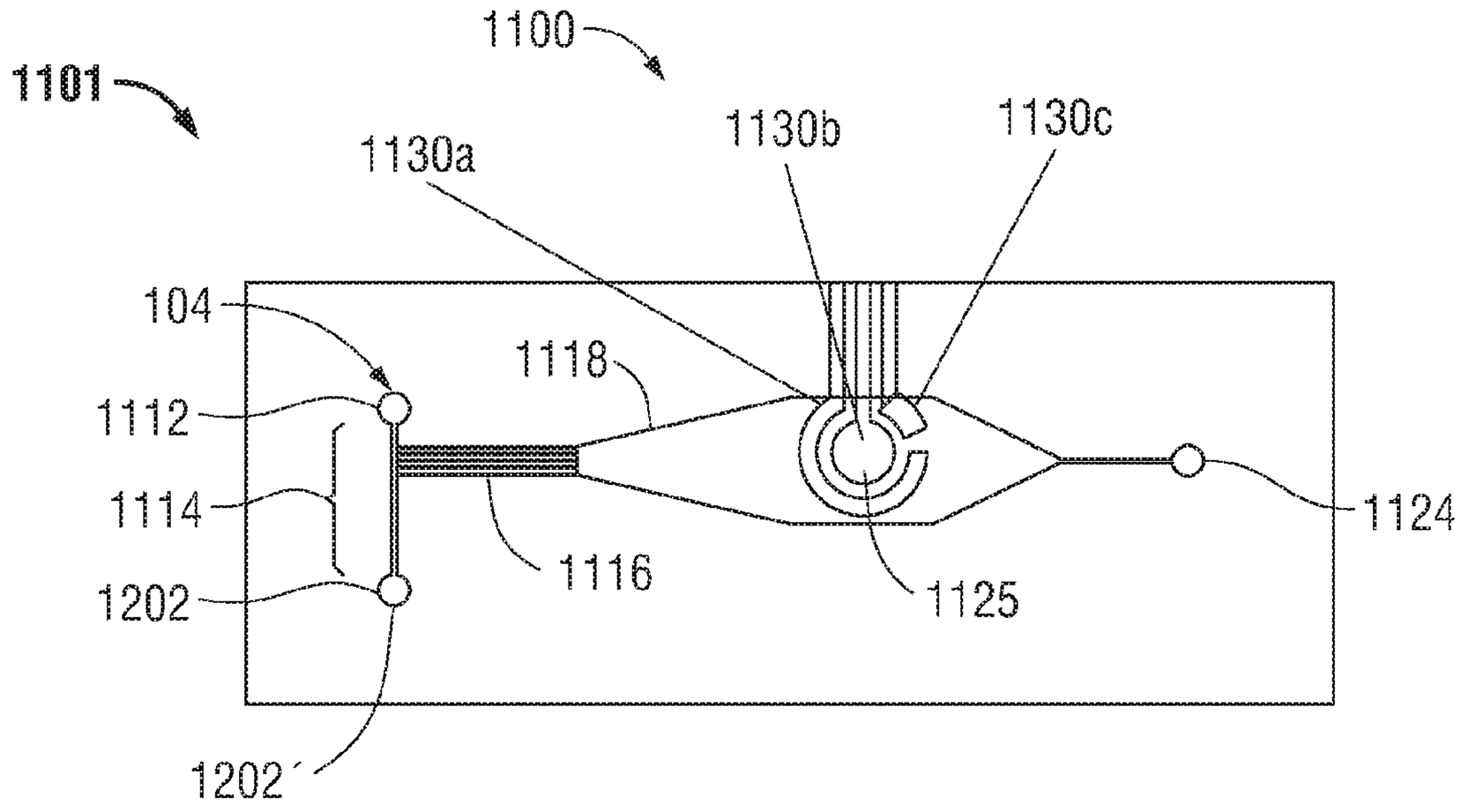
1100
1101
1130a
1130b
1130c
104
1118
1112
1114
1116
1124
1125
1202
1202'

FIG. 2B

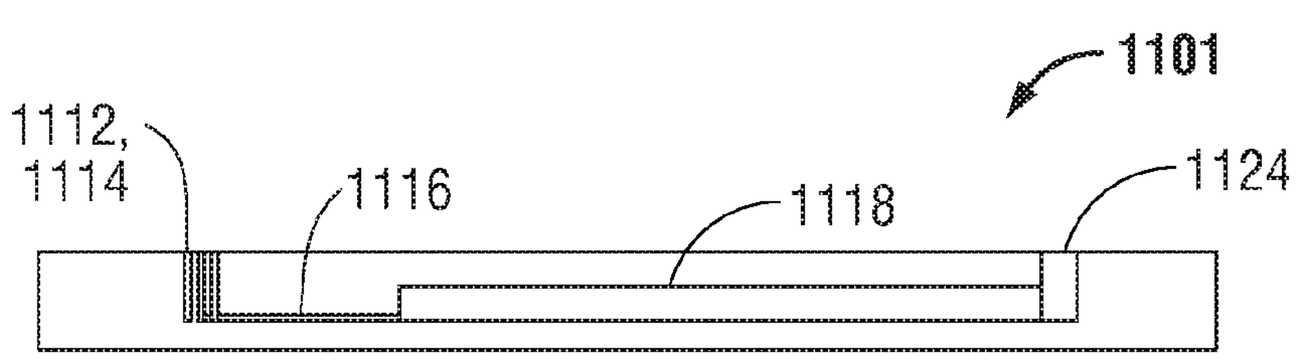
1101
1112,
1114
1116
1118
1124

FIG. 2C

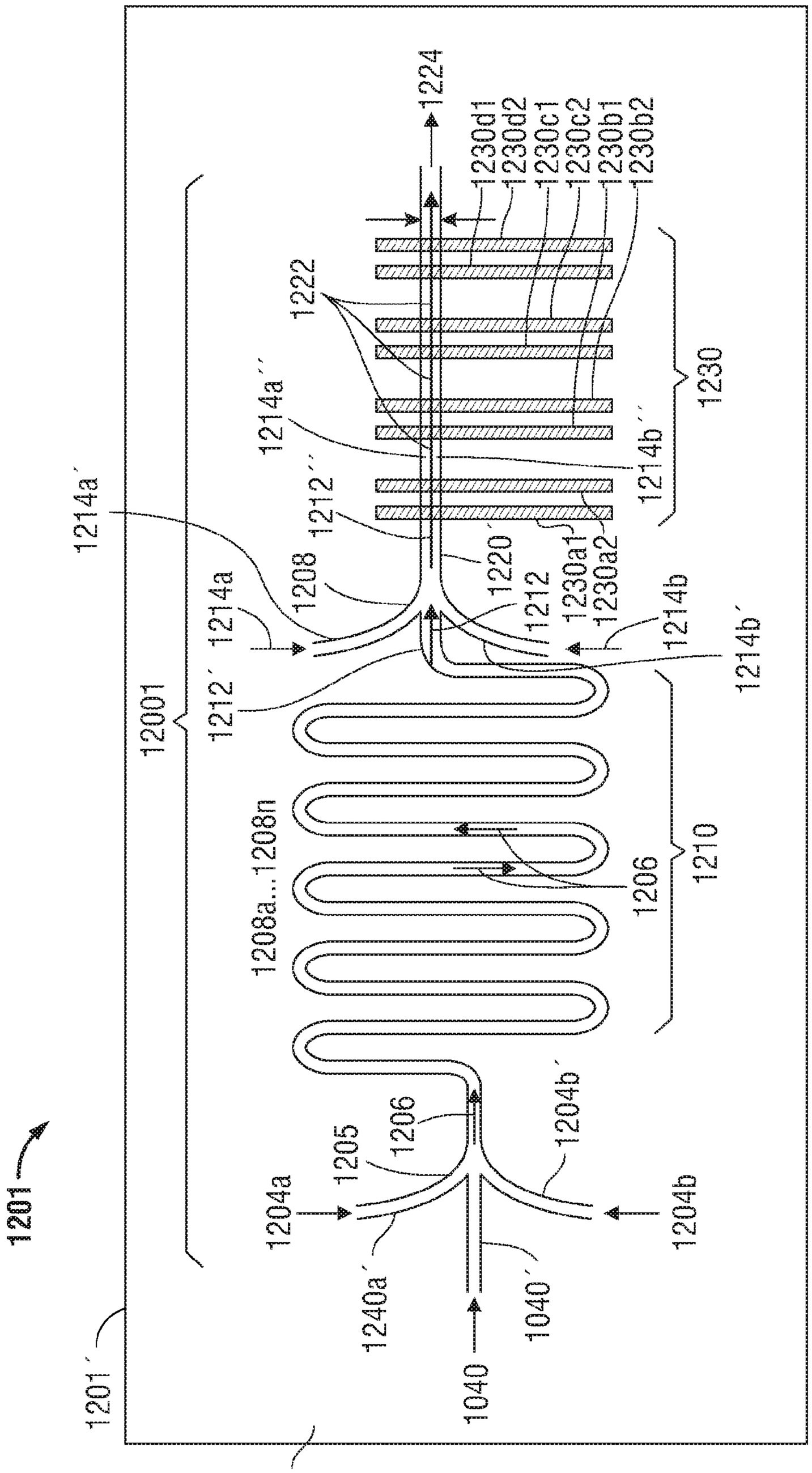
1201
1201´
1203
1204a
1204b
1204b´
1205
1206
1240a´
1040
1040´
1208a...1208n
1208
12001
1210
1212
1212´
1212´´
1214a
1214a´
1214a´´
1214b
1214b´
1214b´´
1220´
1222
1224
1230
1230a1
1230a2
1230b1
1230b2
1230c1
1230c2
1230d1
1230d2

FIG. 3

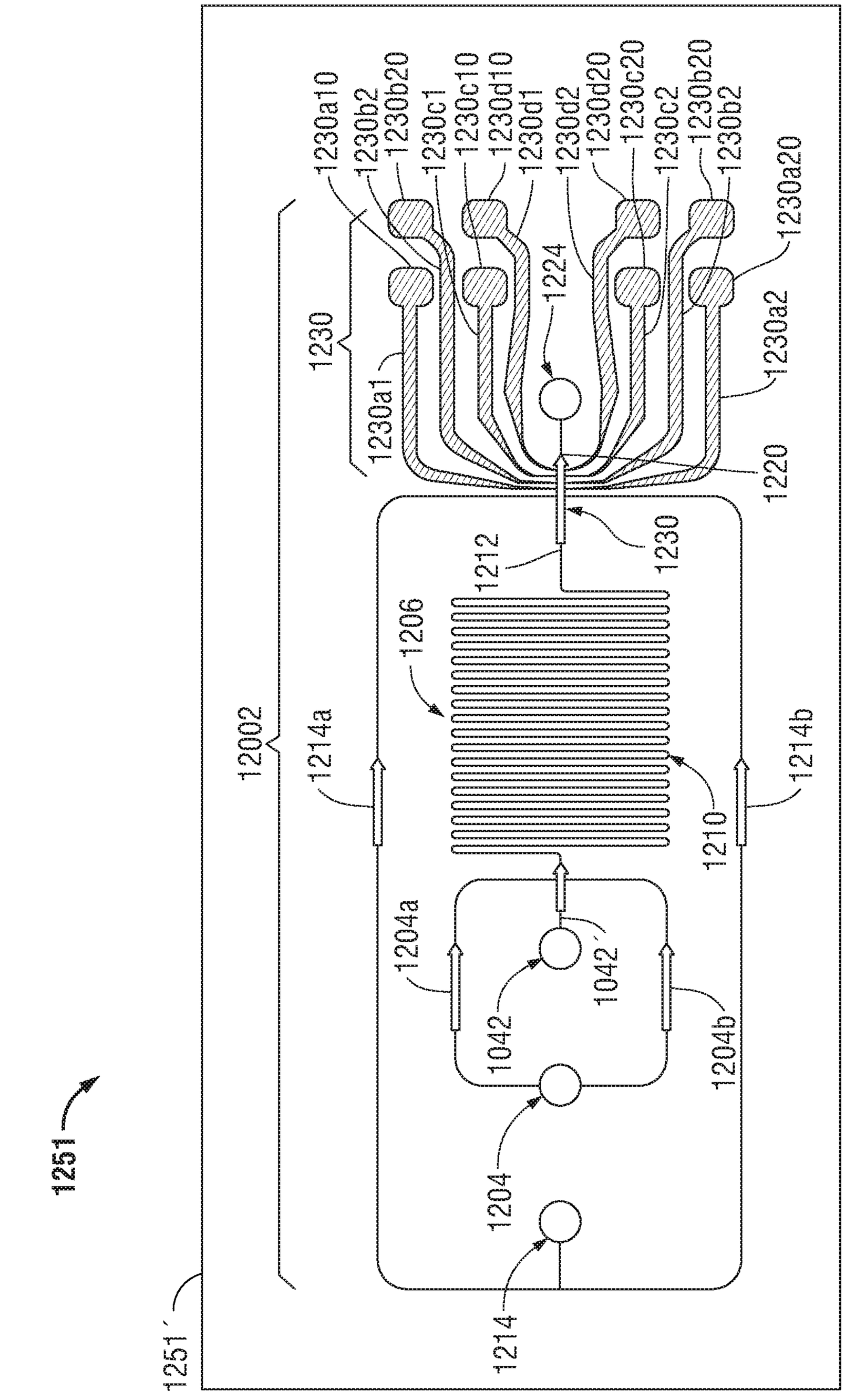
1230a10
1230b2
1230b20
1230c1
1230c10
1230d10
1230d1
1230d2
1230d20
1230c20
1230c2
1230b20
1230b2
1230a20
1230
1224
1230a2
1230a1
1220
1212
1230
1206
12002
1214a
1214b
1210
1204a
1042'
1042
1204b
1204
1214
1251'
1251

FIG. 4

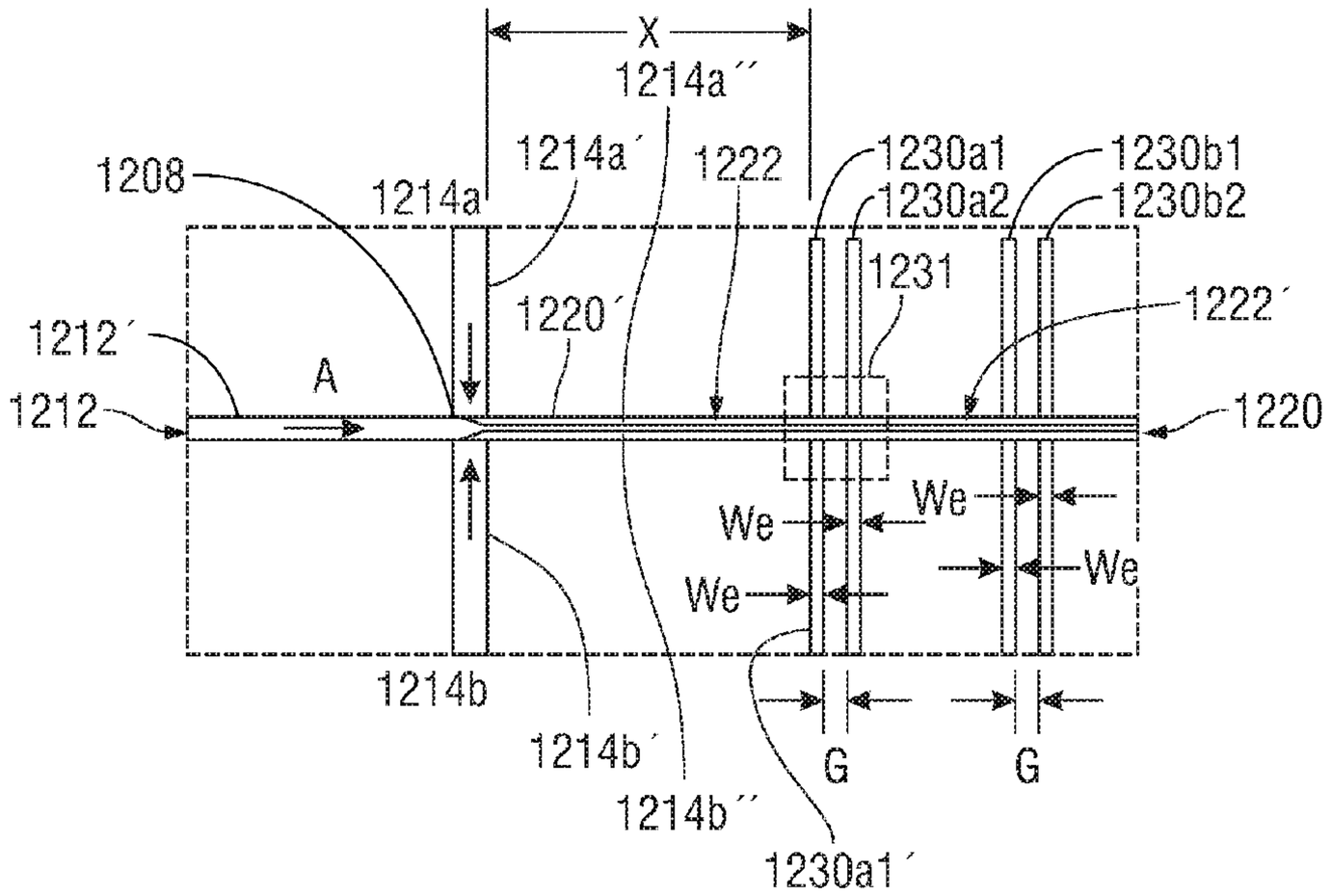
X
1214a''
1214a'
1222
1230a1
1230b1
1230a2
1230b2
1208
1214a
1231
1222'
1220'
1212'
A
1212
1220
We
We
We
We
1214b
1214b'
1214b''
G
G
1230a1'

FIG. 5

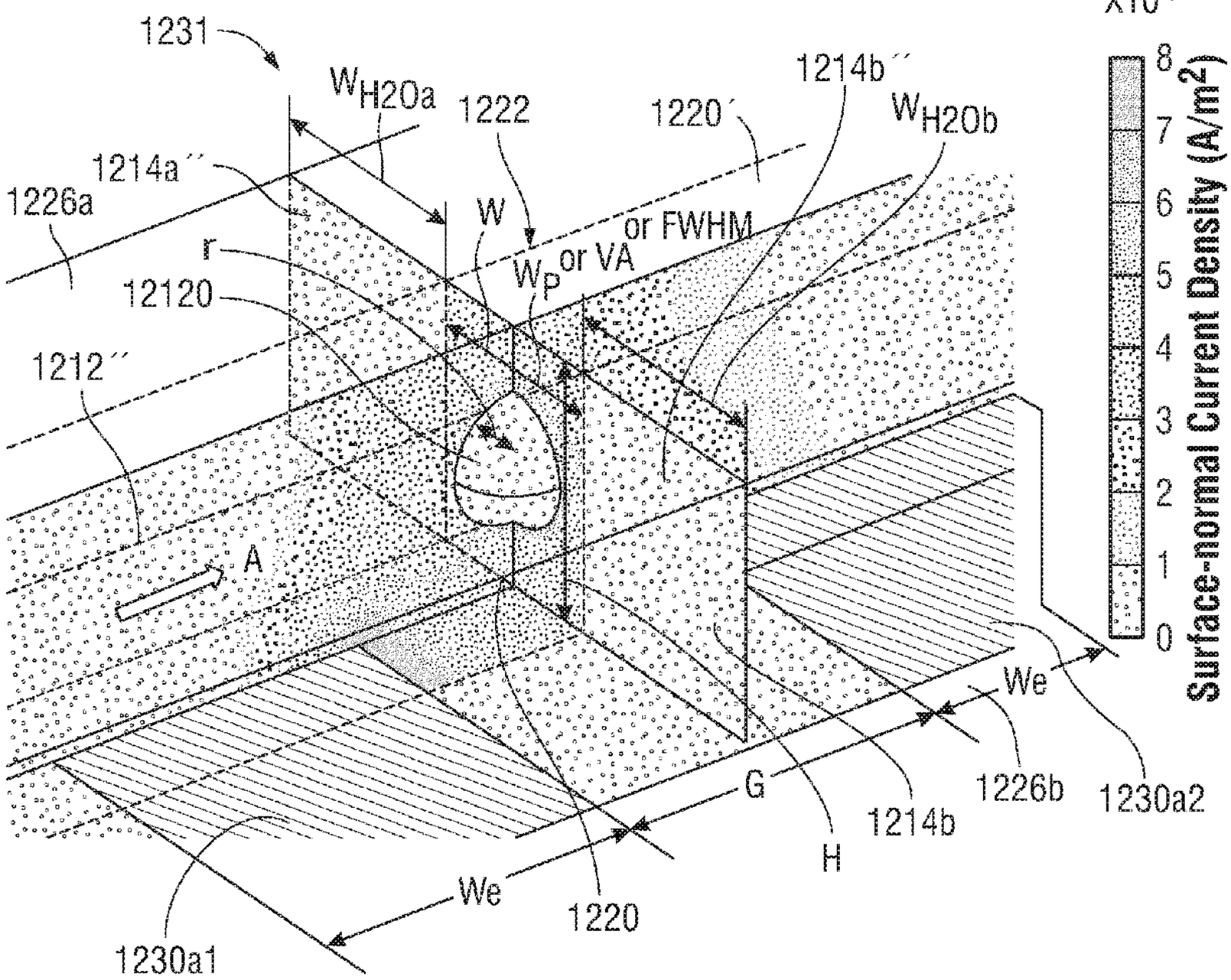
1231
W_{H2Oa}
1222
1220'
1214b''
W_{H2Ob}
1214a''
1226a
W
r
W_P or VA
or FWHM
12120
1212''
A
X10^4
8
7
6
5
4
3
2
1
0
Surface-normal Current Density (A/m²)
We
G
H
1214b
1226b
1230a2
We
1220
1230a1

FIG. 6

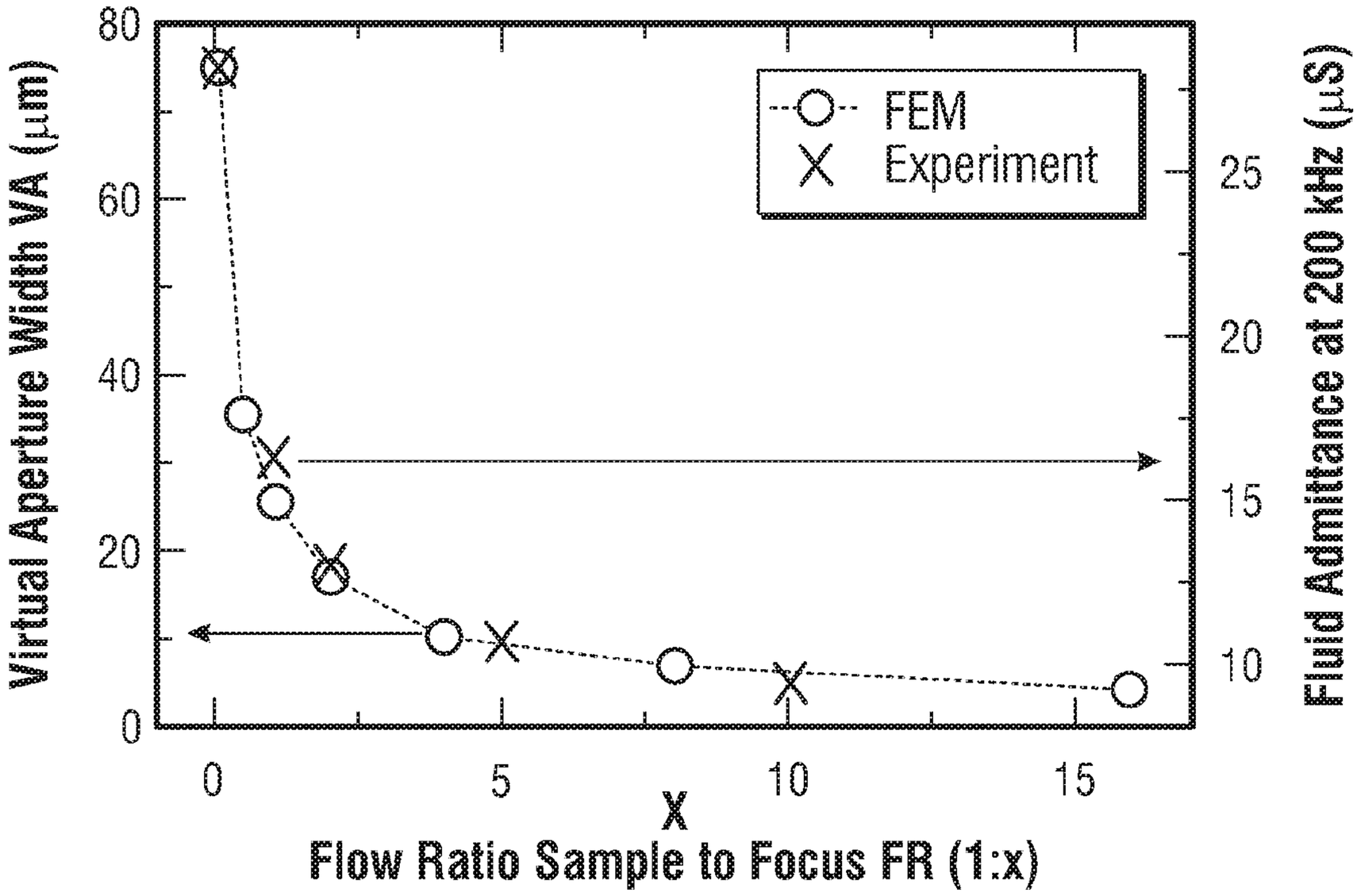
Virtual Aperture Width VA (μm)
Fluid Admittance at 200 kHz (μS)
FEM
Experiment
0
20
40
60
80
0
5
10
15
20
25
X
Flow Ratio Sample to Focus FR (1:x)

FIG. 7

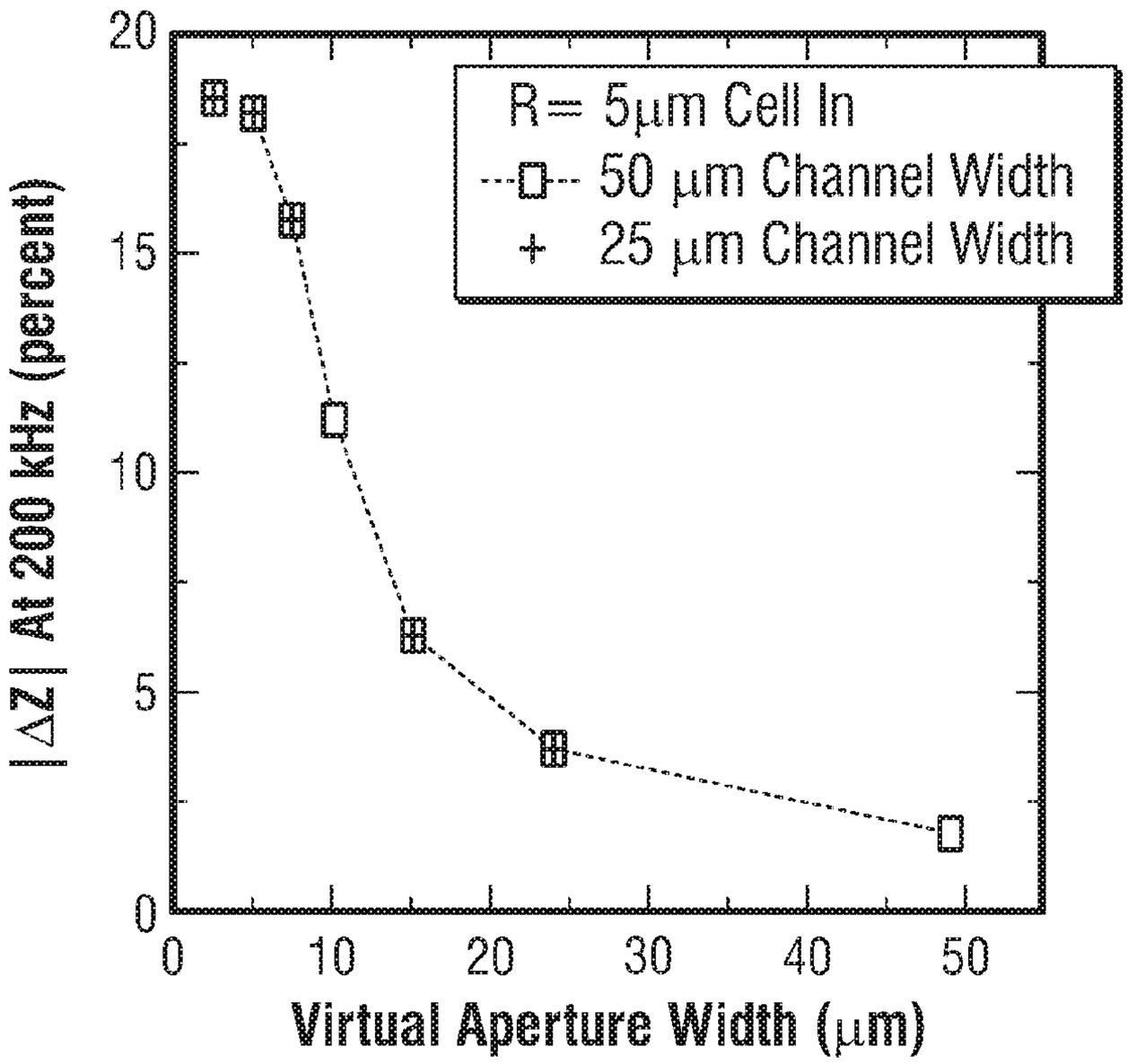
|ΔZ| At 200 kHz (percent)
R= 5μm Cell In
50 μm Channel Width
25 μm Channel Width
0
5
10
15
20
0
10
20
30
40
50
Virtual Aperture Width (μm)

FIG. 8

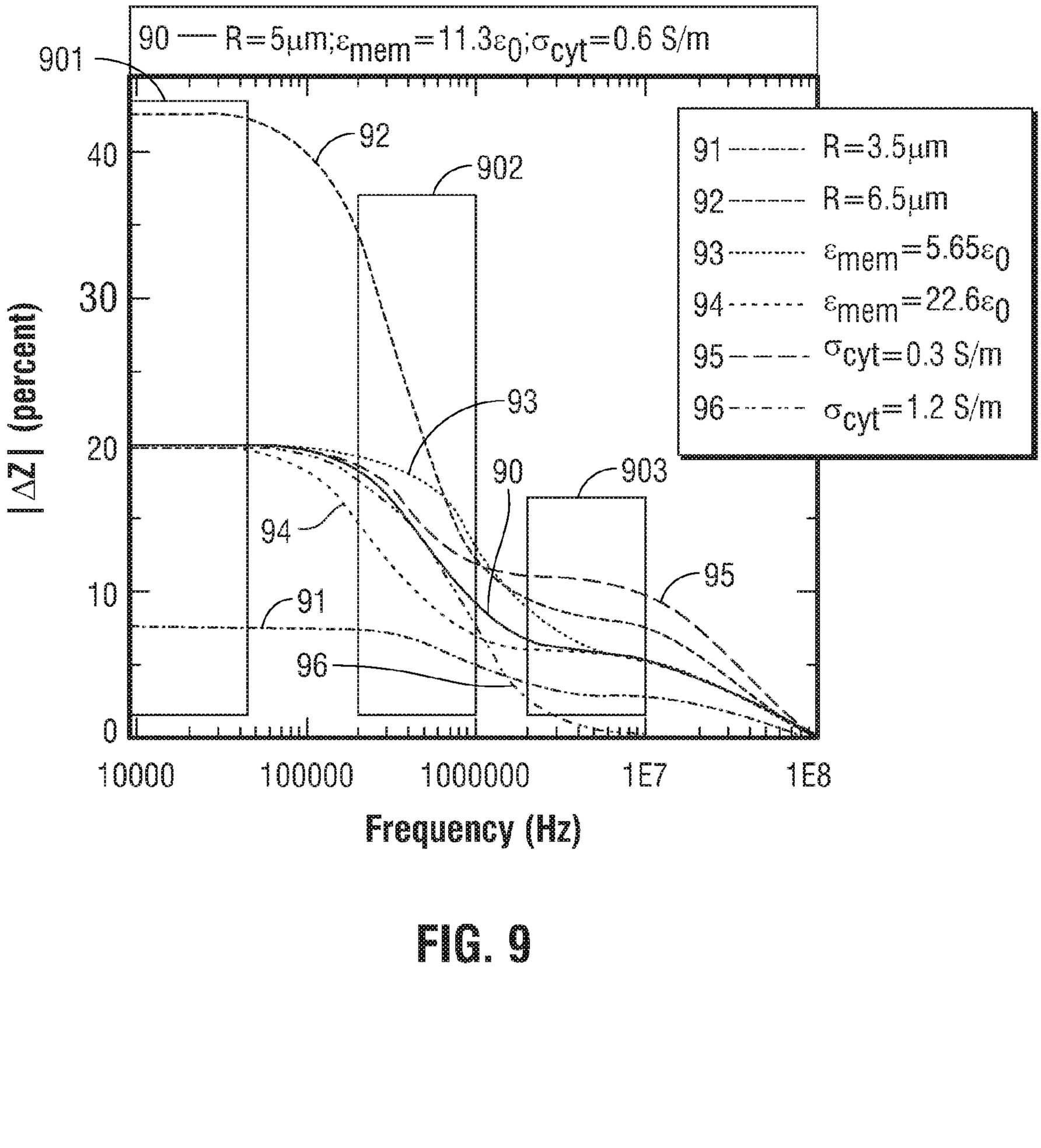
90 R=5μm;εmem=11.3ε0;σcyt=0.6 S/m
901
902
903
91 R=3.5μm
92 R=6.5μm
93 εmem=5.65ε0
94 εmem=22.6ε0
95 σcyt=0.3 S/m
96 σcyt=1.2 S/m
|ΔZ| (percent)
0
10
20
30
40
10000
100000
1000000
1E7
1E8
Frequency (Hz)

FIG. 9

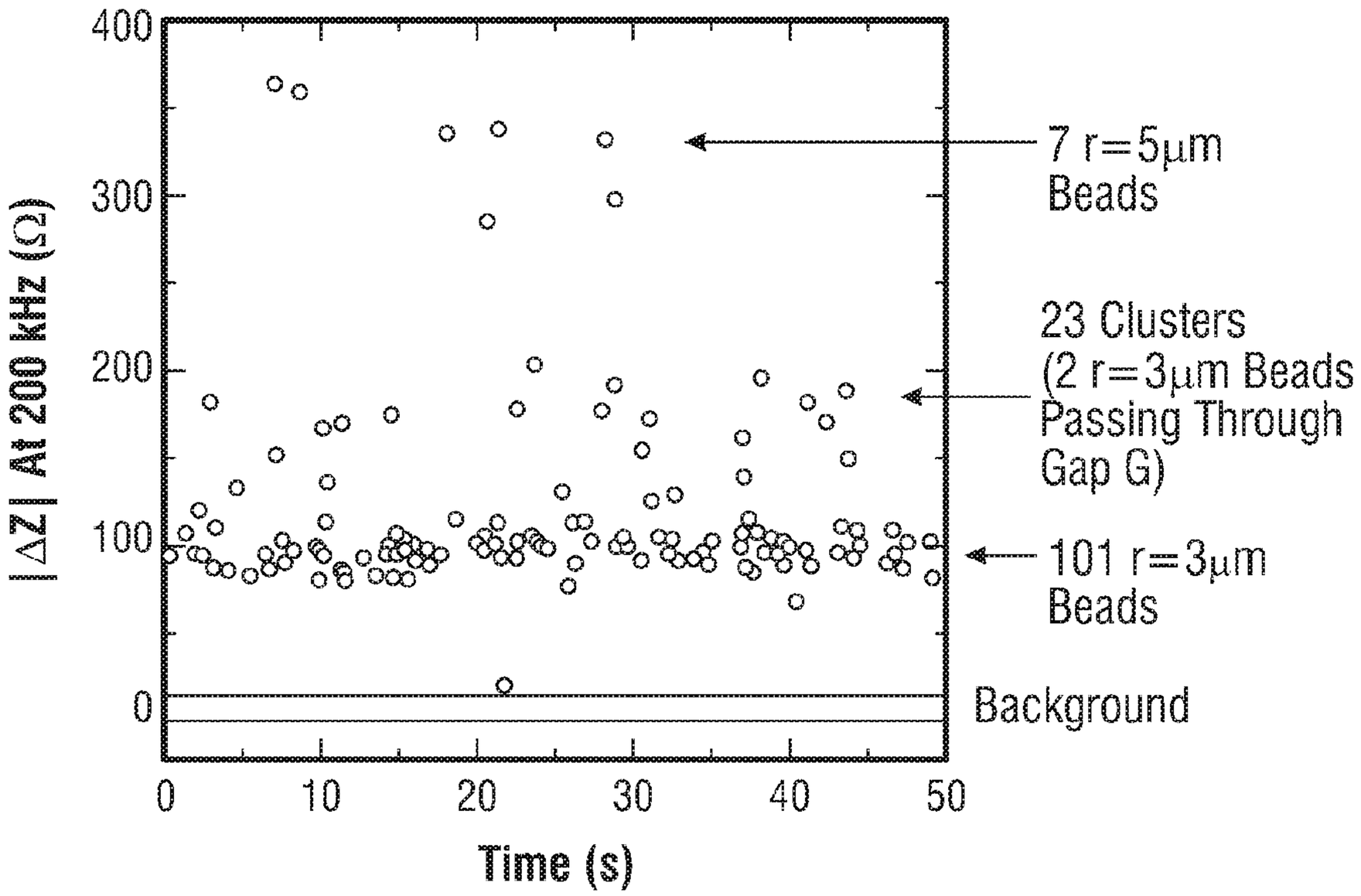
400
300
200
100
0
|ΔZ| At 200 kHz (Ω)
0
10
20
30
40
50
Time (s)
7 r=5μm Beads
23 Clusters (2 r=3μm Beads Passing Through Gap G)
101 r=3μm Beads
Background

FIG. 10

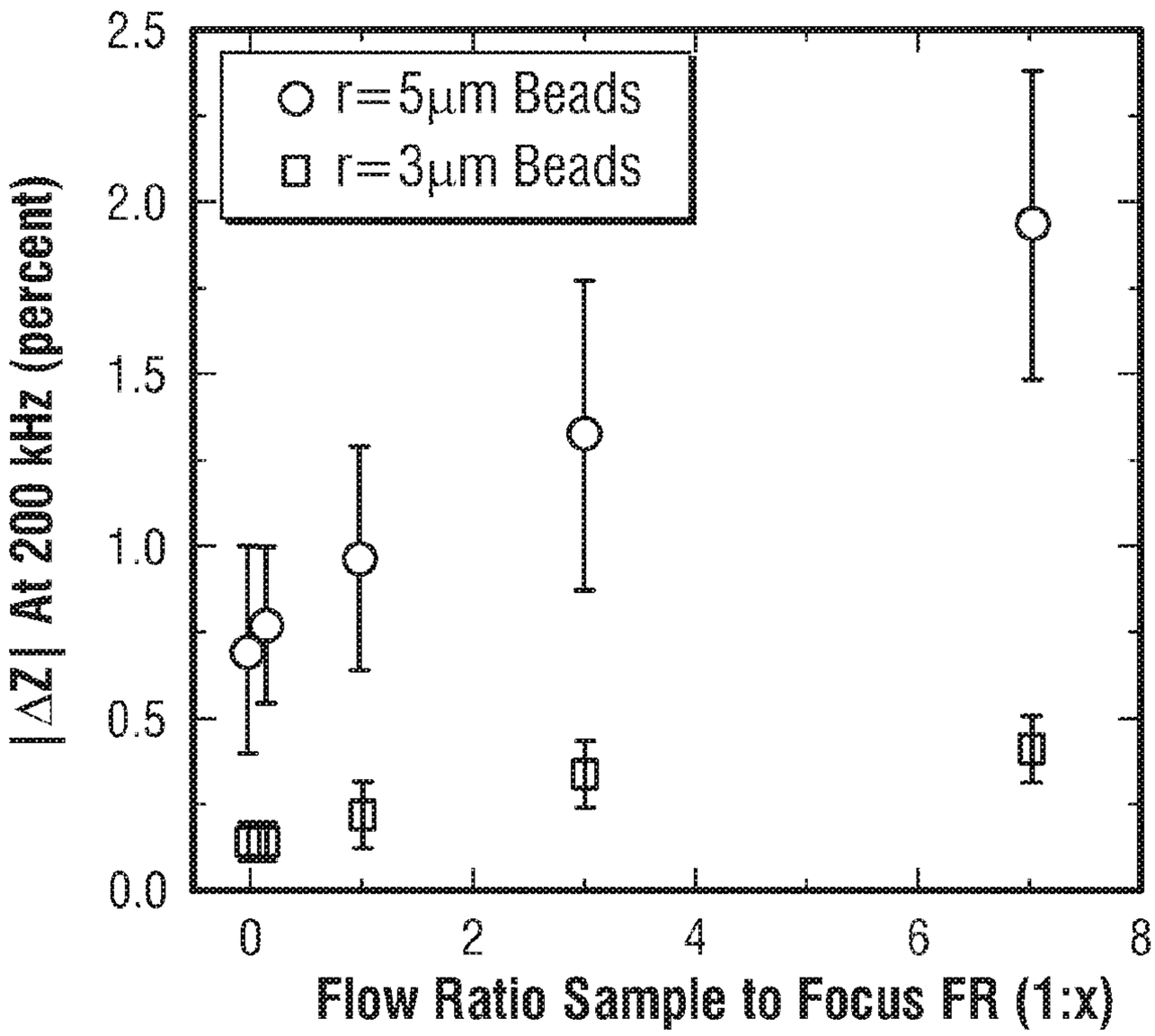
2.5
2.0
1.5
1.0
0.5
0.0
|ΔZ| At 200 kHz (percent)
r=5μm Beads
r=3μm Beads
0
2
4
6
8
Flow Ratio Sample to Focus FR (1:x)

FIG. 11

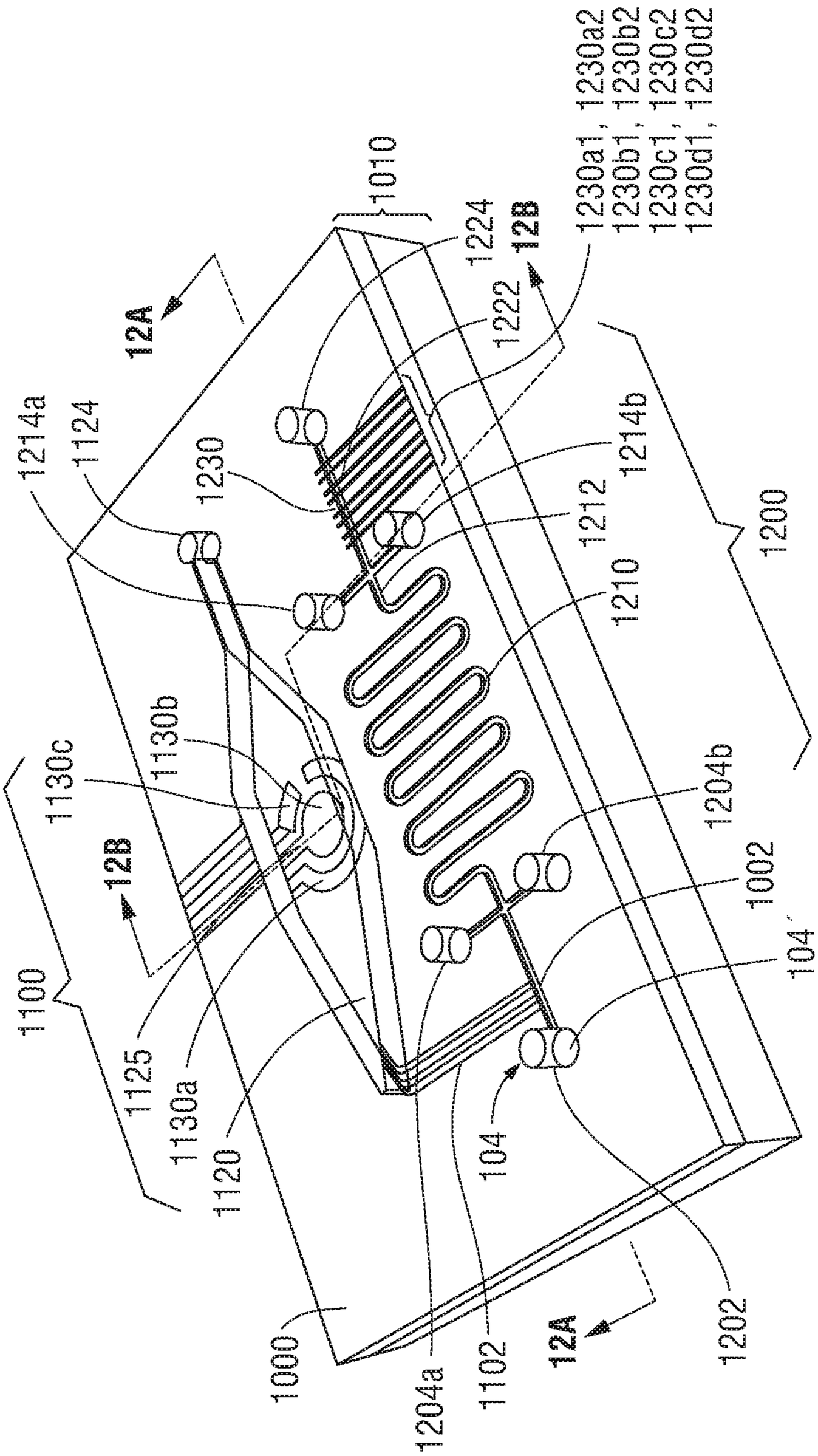
1230a1, 1230a2
1230b1, 1230b2
1230c1, 1230c2
1230d1, 1230d2
1010
1224
12B
1222
12A
12B
12A
1214a
1124
1230
1214b
1212
1210
1200
1130c
1130b
1100
1125
1130a
1120
1204b
1002
104
1000
1204a
1102
1202

FIG. 12

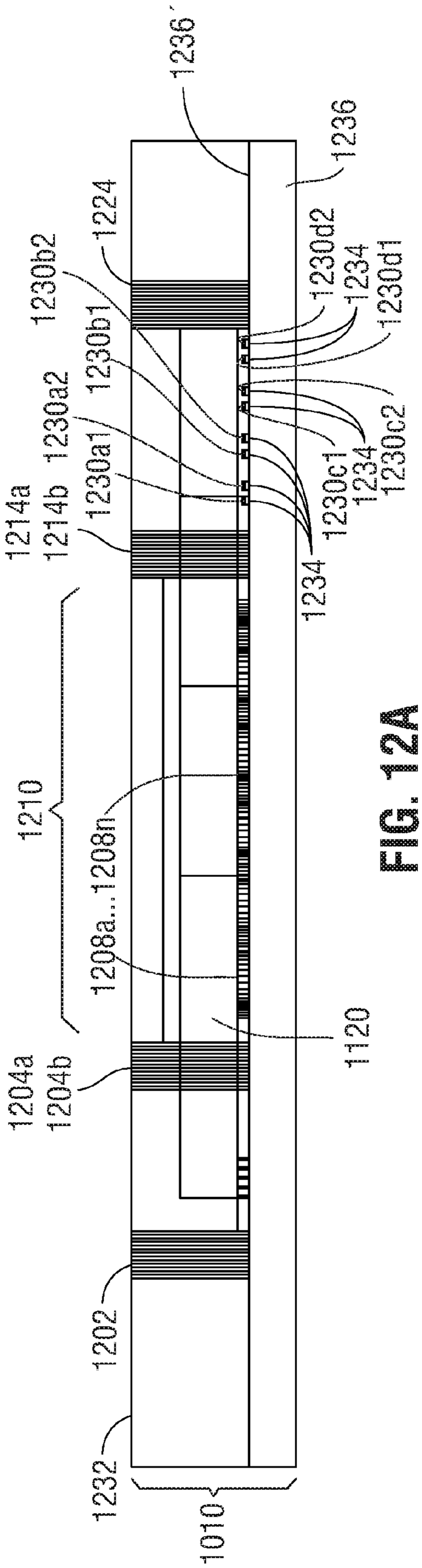

FIG. 12A

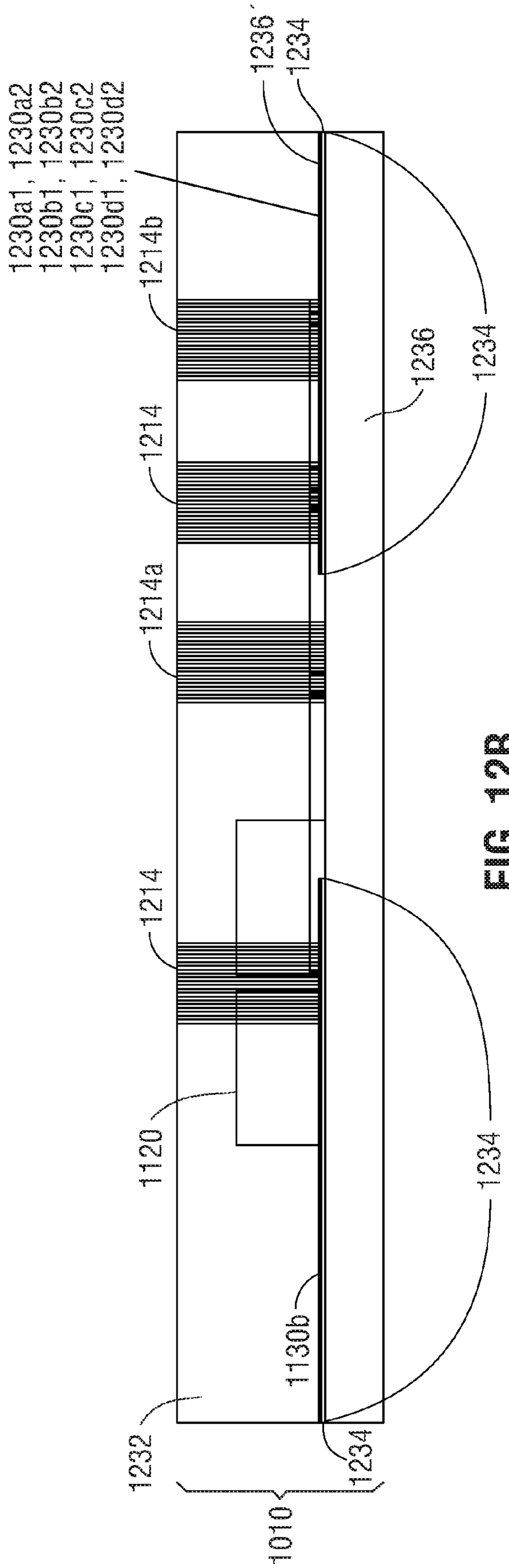

FIG. 12B

INTEGRATED AND STANDALONE LABEL AND REAGENT-FREE MICROFLUIDIC DEVICES AND MICROSYSTEMS FOR DIFFERENTIAL WHITE BLOOD CELL COUNTS

CROSS-REFERENCE TO RELATED APPLICATIONS

[0001] This application claims the benefit of, and priority to, a PCT application, filed on Nov. 17, 2014, entitled "INTEGRATED AND STANDALONE LABEL AND REAGENT-FREE MICROFLUIDIC DEVICES AND MICROSYSTEMS FOR DIFFERENTIAL WHITE BLOOD CELL COUNTS" by Hadar Ben-Yoav et al., which claims priority to U.S. Provisional Patent Application No. 61/905,028, filed on Nov. 15, 2013, entitled "SYSTEM AND METHOD FOR MONITORING DRUG TREATMENT" by Hadar Ben-Yoav et al.; the entire contents of both applications are incorporated by reference herein. These applications relate to U.S. patent application Ser. No. 14/274,643, filed on May 9, 2014, entitled "ANALYTICAL MICRO-DEVICES FOR MENTAL HEALTH TREATMENT MONITORING" by Hadar Ben-Yoav et al., the entire contents of which are incorporated by reference herein. U.S. patent application Ser. No. 14/274,643 claims priority to U.S. Provisional Patent Application No. 61/905,028 and U.S. Provisional Patent Application No. 61/821,344, filed on May 9, 2013, entitled "ANALYTICAL MICRO-DEVICES FOR MENTAL HEALTH TREATMENT MONITORING" by Hadar Ben-Yoav et al. The entire contents of U.S. Provisional Patent Application No. 61/821,344 are incorporated by reference herein.

BACKGROUND

[0002] 1. Technical Field

[0003] The present disclosure relates to the field of detection of substances present in biological fluids. More particularly, the present disclosure relates to devices, systems and methods for detection of analytes and substances in biological fluids such as blood.

[0004] 2. Background of Related Art

[0005] Characterization of large quantities of individual particles is highly relevant to multiple fields, particularly blood analysis [1]. Blood is a highly complex fluid consisting of acellular (plasma) as well as diverse cellular components. The latter can cause significant interference when attempting to detect plasma biomarkers A simple cell count is useful, e.g. to diagnose anemia, but the utility of such measurements increases significantly with the ability to also determine size, surface markers, and interior composition. Applications range from CD4 T-cell monitoring in cases of HIV to stem cell characterization in research. The current gold standard for such measurements is bulky benchtop flow cytometers. These rely on a focused stream of blood cells being subjected to multiple analysis methods, involving fluorescent labels for population-specific surface antigens (e.g. CD4, CD8, . . .), laser light scattering, and absorbance, or impedance measurements. Flow cytometers allow for highly accurate analysis, but rely on labels and complex optics. These factors are some of the major barriers in bringing this technology to the point of care (POC), where it would benefit patients as well as physicians by providing immediate results and increasing accessibility, especially in remote locations [2]. Lab-on-a-chip (LOC) systems have in recent years been shown to provide numerous advantages in clinical diagnostics, including portability, short reaction times, and low sample volumes [2]. These systems aim at bringing tests and procedures currently requiring a centralized laboratory to the POC or even the patient, integrating sample handling, biomarker detection, and readout electronics in a chip-size package.

[0006] Differential blood cell counters are representative examples of microfluidic devices that are already commercially available [3, 4]. However, these devices all rely on chemical reagents to enhance differentiation, and to date no portable POC device achieves a full (five-part) white blood cell differential. An intrinsic advantage here is that the current bench top laboratory methods are already based on microfluidics, and researchers have made efforts to translate these to modular LOC approaches [1, 5-11].

[0007] Especially impedance cytometry is well suited towards integration in microsystems, as it does not rely on labels or complex optics. To date, only few groups have published LOC-based complete white blood cell differentials based on impedance cytometry, including Holmes et al. [23] and Han et al. [24]. The former's approach, however, is limited due to inclusion also of optical measurements (and thus requiring fluorescent labels and external lasers, lenses, etc.), chemical reagents to enhance white blood cell differentiation, and an exceedingly complex fabrication method. The latter forgo optical measurements, but still rely on chemical reagents and suffer from inadequate differentiation.

[0008] Impedance cytometry in its most basic form applies the Coulter principle. As a particle (or cell) of diameter dp passes through an aperture of diameter DA between two chambers, it causes a change in impedance ΔZ measured between two electrodes on either side of the aperture. A first-order approximation for this change is $\Delta Z=4\rho_m d_p^3/\pi D_A^4$, where ρ_m is the resistivity of the electrolyte.

[0009] Consequently, this signal can be used to differentiate particles based on their size. This is useful for blood cell differentials, as there are significant differences in geometry—discoid red blood cells with 6-8 μm diameters, compared to spherical white blood cells with diameters ranging from 6-20 μm for the various sub-populations. Red blood cells, outnumbering white blood cells approximately 1000:1, all but prohibit an accurate count of different leukocyte subtypes in whole blood. More elaborate implementations of the impedance method can give additional information about the cells: while direct current (DC) or low frequency alternating current (AC) impedance is sensitive to size, higher frequency AC probes the internal structure of the cell. Leukocyte subpopulations can be distinguished by combining these modes, especially when the much more numerous erythrocytes are lysed by addition of chemical reagents to reduce interference. Recently, an integrated LOC system based on impedance cytometry has been shown to be capable of quantifying the different types of blood cells, including neutrophils [12, 13]. A notable limitation is the reliance on chemicals to achieve erythrocyte lysis and sufficient cell type differentiation (saponin and formic acid, followed by sodium carbonate after a set exposure time).

[0010] Extending into the alternating current domain allows for probing more generalized changes in dielectric properties caused by particles within the interaction volume [3].

[0011] Multi-frequency impedance cytometry has been presented as an attractive method for multi-dimensional single-cell analysis in LOC systems [4], [5]. However, current

implementations still suffer from limited resolution, and employ multi-layer fabrication processes. While flow focusing has been utilized to enhance the performance of coulter counter-type devices, to date no systematic study has been conducted on the interplay between flow ratios, particle sizing sensitivity, and throughput [6]. It is only through such studies, both in models and experiments, that optimal utilization of microsystem capabilities becomes possible.

SUMMARY

[0012] The embodiments of the present disclosure provide a novel and non-obvious solution to the problems of mental health treatment as described above by providing a point of care testing (POCT) device that includes a whole blood inlet port in fluidic communication with microchannels extending therefrom.

[0013] The embodiments of the present disclosure provide a point of care testing (POCT) device that limits the amount of required chemicals, as additional reagents complicate LOC packaging.

[0014] The embodiments of the present disclosure provide a point of care testing (POCT) device that eliminates the need for multi-layer fabrication processes that represent a practical drawback in terms of scale-up.

[0015] The embodiments of the present disclosure provide reagent- and label-free assay (only water) in conjunction with impedance cytometry.

[0016] Integration of pure water hydrodynamic focusing to enhance signal-to-noise ratio.

[0017] Integration of pure water erythrocyte lysis to eliminate background signal and enhance white blood cell differentiation.

[0018] Two-layer design with polydimethylsiloxane (PDMS) channels and coplanar gold electrodes on glass for simple, low-cost fabrication.

[0019] Consequently, one embodiment of the present disclosure relates to a method of establishing a differential white blood cell count that includes directing at least one stream of deionized water into a microfluidic device containing a sample of whole blood of a subject or a cell-rich fraction of a whole blood sample or a cell-free fraction of whole blood of a subject or combinations thereof to generate a lysate stream of intact white blood cells; directing at least one stream of deionized water into the lysate stream such that the lysate stream with intact white blood cells is forced to flow in a direction of motion by the at least one stream of deionized water to form a virtual non-conductive aperture in a channel of the microfluidic device; and performing impedance cytometry of the lysate stream in the virtual non-conductive aperture via coplanar electrodes to detect the presence of intact white blood cells in the lysate stream.

[0020] The method may further include quantitatively differentiating between neutrophils, lymphocytes, monocytes, eosinophils, and basophils in the lysate stream based on the impedance measurements resulting from the performance of the impedance cytometry.

[0021] Additionally, the step of directing at least one stream of deionized water into the channel may include symmetrically focusing at least two streams of deionized water orthogonally on opposing sides of the direction of motion of the lysate stream to form the virtual non-conductive aperture.

[0022] Yet another embodiment of the present disclosure relates to a method of fabricating a microfluidic device that include forming a layer of material on a substrate and adhering a plurality of pairs of co-planar electrodes on the substrate; and forming a plurality of microchannels in the layer of material. At least one of the microchannels is configured and disposed to receive at least one stream of deionized water to effect lysis of a whole blood sample or of a cell-rich fraction of a whole blood sample to produce a lysate stream. At least one of the microchannels is configured and disposed to receive the lysate stream and to receive at least one focusing flow of deionized water to effect a virtual aperture. At least one the pairs of co-planar electrodes is formed under one of the plurality of microchannels in which is generated the virtual aperture such that impedance cytometry of the lysate stream in the virtual aperture is enabled by application of an electric field to at least two pairs of the plurality of pairs of co-planar electrodes.

[0023] The step of adhering a plurality of pairs of co-planar electrodes on the substrate may include applying a chrome adhesive between the plurality of pairs of co-planar electrodes and the substrate.

[0024] Still another embodiment of the present disclosure relates to a microfluidic device that includes a layer of material formed over a substrate. A blood separation section is configured and disposed in the layer of material to receive a sample of whole blood of a subject and to separate the whole blood sample into a cell-free fraction and into a cell-rich fraction. An analyte sensor section is configured and disposed in the layer of material to detect an analyte in the cell-free fraction via application of an electrical field and detection of changes in at least one electrical property in the analyte. A cell pre-treatment section is configured and disposed in the layer of material to form a lysate from the cell-rich fraction; and a cell or large particle analyzer section configured and disposed on the layer of material to enable analysis of the lysate from the cell-rich fraction to detect circulating tumor cells or white blood cells including neutrophils, lymphocytes, monocytes, eosinophils, and basophils.

[0025] The cell or large particle analyzer section may be configured and disposed on the layer of material to enable analysis of the lysate from the cell-rich fraction to enable a differential white blood cell count via coplanar electrodes formed over the substrate that are configured and disposed to enable impedance cytometry of the white blood cells in the cell or large particle analyzer section.

[0026] A further embodiment of the present disclosure relates to a microfluidic device for establishing a differential white blood cell count that includes a substrate. A layer of material is formed over the substrate and a plurality of microchannels is formed in the layer of material. At least one of the plurality of microchannels is configured and disposed to receive a sample of whole blood of a subject or a cell-rich fraction of a whole blood or combinations thereof. At least one of the plurality of microchannels is configured and disposed to receive at least one stream of deionized water to effect lysis of a whole blood sample or of a cell-rich fraction of a whole blood sample to produce a lysate stream. At least one of the plurality of microchannels is configured and disposed to receive the lysate stream and to receive at least one focusing flow of deionized water to effect a virtual aperture. At least one the pairs of co-planar electrodes is formed under one of the plurality of microchannels in which is generated the virtual aperture such that impedance cytometry of the lysate stream in the virtual aperture is enabled by application of an electric field to at least two pairs of the plurality of pairs of co-planar electrodes.

[0027] With respect to the at least one of the plurality of microchannels that is configured and disposed to receive the lysate stream and to receive at least one focusing flow of deionized water to effect a virtual aperture, the plurality of microchannels may include at least two deionized water injection channels and a lysate stream channel such that the at least two deionized water injection channels are configured and disposed to symmetrically focus at least two streams of deionized water orthogonally on opposing sides of a direction of motion of the lysate stream in the lysate stream channel.

BRIEF DESCRIPTION OF THE DRAWINGS

[0028] These and other advantages will become more apparent from the following detailed description of the various embodiments of the present disclosure with reference to the drawings wherein:

[0029] FIG. **1** illustrates a flow chart of an integrated cell-free and cell-rich fraction microfluidic device and testing interface for implementing a method of testing a cell-free fraction and a cell-rich fraction of a whole blood sample of a patient or subject;

[0030] FIG. **2**A is a perspective view of a microfluidic device that is functionally independent of the integrated microfluidic device of FIG. **1** but is functionally equivalent to the cell-free fraction analysis section of the integrated microfluidic device of FIG. **1**;

[0031] FIG. **2**B is a plan view of the microfluidic device of FIG. **2**A;

[0032] FIG. **2**C is a cross-section view of the microfluidic device of FIG. **2**A taken along section line **2**C-**2**C;

[0033] FIG. **3** illustrates a microfluidic device that is also physically independent of the integrated microfluidic device of FIG. **1** but which is functionally equivalent to the cell-rich fraction analysis section of the integrated microfluidic device of FIG. **1**;

[0034] FIG. **4** illustrates an alternate embodiment of the microfluidic device of FIG. **3**;

[0035] FIG. **5** illustrates one embodiment of a portion of the whole blood analysis section of the microfluidic devices illustrated in FIG. **3** and FIG. **4**;

[0036] FIG. **6** illustrates a 3-dimensional electrodynamic model that simulates a particle of the lysate stream of FIG. **5** in a section of microfluidic channel which defines first and second vertical channel walls wherein the particle is suspended in the gap between two coplanar electrodes;

[0037] FIG. **7** is a plot of virtual aperture width and fluid admittance plotted against flow ratio sample to focus;

[0038] FIG. **8** is a plot of the absolute value of the change in impedance $|\Delta Z|$ at 200 kHz as a percentage with respect to the empty channel impedance plotted against virtual aperture width;

[0039] FIG. **9** is a finite element model simulation of the absolute value of the change in impedance in percent for a cell with given properties represented by a radius, membrane capacitance and cytosol conductivity, and single-parameter variations thereof illustrating three distinct frequency regimes where an increase or decrease significantly alters the signal;

[0040] FIG. **10** is a plot of impedance at 200 kHz in ohms corresponding to particles passing between the electrodes as a function of time in seconds;

[0041] FIG. **11** is a plot of the average impedance at 200 kHz in percent for separate bead populations as a function of flow ratio sample to focus;

[0042] FIG. **12** illustrates a perspective view of one embodiment of the integrated microfluidic device described schematically with respect to FIG. **1**

[0043] FIG. **12**A is a cross-sectional view of the microfluidic device of FIG. **12** taken along section line **12**A-**12**A; and

[0044] FIG. **12**B is a cross-sectional view of the microfluidic device of FIG. **12** taken along section line **12**B-**12**B.

DETAILED DESCRIPTION

[0045] A microfluidic device relying solely on impedance measurements to establish a differential white blood cell_count as disclosed herein introduces a number of improvements over previous designs. The design according to embodiments of the present disclosure employs coplanar electrodes, simplifying device assembly as compared to parallel electrodes not least by reducing the number of physical layers from three to two. Furthermore, the flow channels are defined in polydimethylsiloxane (PDMS) fabricated by established molding techniques. This straightforward approach again eliminates complexity over the use of photolithographically patterned polyimide and micromilled polymethyl methylacrylate (PMMA).

[0046] Rather than employing chemical reagents to eliminate erythrocyte interference as well as enhance leukocyte differentiation, pure water is employed. For eventual clinical application, limiting the amount of required chemicals is an important consideration. Exposure of the cell stream to pure water creates a strong osmotic gradient across plasma membranes, causing swelling and ultimately lysis [18], [19]. White blood cells are much more resistant to osmotic gradients than red blood cells, with neutrophils surviving more than three times as long as erythrocytes [20].

[0047] To accommodate osmotic lysis on chip, similar to the design employed by Zhan et al. to study the phenomenon, streams of pure water are symmetrically introduced to the sample flow a certain distance prior to the electrodes [19]. The distance and flow speeds are tuned such that the osmotic stress exposure prior to impedance cytometry results in lysis of red, but not white, blood cells. The osmotic swelling experienced by the leukocytes is also expected to heterogeneously affect sub-populations such as to further enhance differences probed by impedance cytometry.

[0048] The loss in performance by utilizing coplanar compared to parallel electrodes is about 20%, notably decreasing for increasing cell size [15]. To retain or exceed the performance demonstrated by e.g. Holmes et al. channels with smaller dimensions are employed herein, and thus smaller equivalent aperture DA, than their 40×40 μm^2. The channel height are comparable to the white blood cell diameters at below 20 μm, thus also reducing the impact of vertical cell position in the flow on the measured signal [15]. Lateral constraint is provided not by the channel itself, but rather by sheath flow focusing. This phenomenon relies on laminar flow and introduction of fluid streams to either side of the sample stream to force central alignment of cells [17]. Providing a virtual aperture, in contrast to physical channel confinement, limits the danger of channel clogging [7], [10]. Although the lysis flows have a similar effect close to their introduction to the main sample flow, that focusing effect wears off over the length of the channel. Separate flows also allow for independent adjustment of parameters for lysis and focusing.

[0049] In summary, a microsystem is disclosed that relies on impedance measurements to establish a differential white

blood cell count, introducing a number of improvements over previous designs. The microsystem enables a method for separating whole blood into a cellular component for neutrophil counting and an undiluted acellular component for analyte detection.

[0050] The overall design, incorporating a main sample flow, pure water lysis flows, focusing flows, and impedance cytometry, is schematically illustrated in FIG. **1** and is described in more detail below. Gold coplanar electrodes may be photolithographically patterned on glass, via a chrome adhesive therebetween, and SU-8 photoresist may be used to create a negative master structure on silicon. Positive PDMS microfluidics can thus be molded and cured, and subsequently bonded to the glass reversibly by simple application of pressure, or permanently by prior application of oxygen plasma. The impedance measurements rely on four sequential sets of coplanar parallel electrode pairs—one for direct current (DC) measurements, one for high-frequency alternating current (AC) measurements, the other two as respective references. The references serve to account for the impedance from the acellular component at both DC and AC frequencies, assuming a cell density resulting in spacing between individual cells larger than the electrode gap. At a known flow rate, the different measurements can be correlated for each cell. Sample flow is provided by pressure actuation from external syringe pumps, connected through capillary tubing. The channels are pre-treated with bovine serum albumin (BSA) protein to reduce sticking of blood cells to the highly hydrophobic PDMS.

[0051] Embodiments of the microsystem of the present disclosure enable a decrease in fabrication complexity and in reliance on chemicals through a coplanar electrode design and reliance on pure water to lyse erythrocytes, respectively.

[0052] Embodiments of the microsystem of the present disclosure incorporate flow focusing of the white blood cell enhanced fraction via hydrodynamic effects of pure water to create a "virtual aperture" to achieve increased, tunable cell characterization performance and throughput.

[0053] The present disclosure of an impedance-based microsystem/microdevice for differential white blood cell counts has the following novel features:

[0054] Reagent- and label-free assay (only water).

[0055] Integration of pure water hydrodynamic focusing to enhance signal-to-noise ratio.

[0056] Integration of pure water erythrocyte lysis to eliminate background signal and enhance white blood cell differentiation.

[0057] Two-layer design with PDMS channels and coplanar gold electrodes on glass for simple, low-cost fabrication.

[0058] Thus, embodiments of the present disclosure of a microsystem relying on impedance measurements to establish a differential white blood cell count introduce a number of improvements over previous designs, such as a decrease in fabrication complexity and a decrease in reliance on chemicals through a coplanar electrode design and instead reliance on pure water to lyse erythrocytes, respectively. At the same time, by incorporating flow focusing, increased, tunable cell characterization performance and throughput are achieved.

[0059] Turning first to FIG. **1**, there is illustrated a flow chart of an integrated cell-free and cell-rich fraction microfluidic device and testing interface **100** for implementing a method of testing a cell-free fraction and a cell-rich fraction of a whole blood sample of a patient or subject. More particularly, the integrated device and testing interface **100** includes a patient or subject **102**.

[0060] As defined herein, cell-free fraction refers to a blood sample from which at least 99% of cellular components such as erythrocytes and leukocytes have been removed from a whole blood sample leaving a plasma of less than 1% cellular composition.

[0061] As defined herein, cell-rich fraction refers to a whole blood sample from which 20% or less of plasma volume has been removed, leaving a sample containing 99% of cellular components such as erythrocytes and leukocytes, potentially concentrated with respect to typical whole blood.

[0062] As defined herein, white blood cells, also referred to as leukocytes, include neutrophils, lymphocytes, monocytes, eosinophils, and basophils, each of which may exist independently in a whole blood sample or cell-rich fraction.

[0063] The method includes extracting or receiving a whole blood sample **104** from the patient or subject **102** and directing the whole blood sample **104** to a blood separation section **1002** of integrated cell-free fraction analysis and cell-rich fraction analysis microfluidic device **1000**. The whole blood sample **104** may be directed to the intake of the blood separation section **1002** via generally one micropump **105** that may be externally positioned with respect to the microfluidic device **1000**, as shown schematically in FIG. **1**, or embedded within the microfluidic device **1000** (not shown). The method includes, via the whole blood sample separation section **1002**, separating the whole blood sample **104** into a cell-free fraction **1102** and into a cell-rich fraction **1202**. The method includes directing the cell-free fraction **1102** to a cell-free fraction analysis section **1100** of microfluidic device **1000** and directing the cell-rich fraction **1202** to a cell-rich fraction analysis section **1200** of the microfluidic device **1000**. As described in more detail below with respect to FIG. **2**, the method of testing includes sensing in the cell-free fraction analysis section **1100** an analyte or biomarker **1125** such as, e.g, a drug or pharmaceutical, metabolites, vitamins, viruses, bacteria, hormones, enzymes, inflammatory mediators, chemokines, immunoglobulin isotypes, intracellular signaling molecules, apoptotic mediators, adhesion molecules, and antibodies etc. (Morgan et al., Clinical Immunology 2004 March; 110(3) 252-66) via an analyte or biomarker sensor **1110** and directing analyte or biomarker analysis results **1140** as all or part of point-of-care information **106** provided by the microfluidic device **1000**. The method of testing also may include directing the cell-rich fraction **1202** to a cell pre-treatment sub-section **1210** of cell-rich analysis section **1200** wherein pre-treatment may include lysis of the cell-rich fraction **1202**, directing the lysate with intact white blood cells **1220** to a cell or large particle analyzer sub-section **1230** and directing impedance cytometry results **1240** as all or part of point-of-care information **106** provided by the microfluidic device **1000**. The cell or large particle analyzer sub-section **1230** may detect white blood cells (or leukocytes) which include various sub-types such as neutrophils, lymphocytes, monocytes, eosinophils, and basophils, or circulating tumor cells or both white blood cells and circulating tumor cells. The cell or large particle analyzer sub-section **1230** excludes detection of red blood cells since such cells do not survive the lysis process that occurs in cell pre-treatment sub-section **1210**.

[0064] The integrated device and testing interface **100** may further include directing the part of point-of-care information

106 to a treatment team of medical professionals or researchers **108** who may direct an adjustment in action plan **110** for the patient or subject **102**.

[0065] FIGS. **2**A, **2**B and **2**C illustrate in more detail the cell-free fraction analysis section **1100** of microfluidic device **1000** which includes analyte or biomarker sensor **1110** for detecting an analyte or biomarker in cell-free fraction **1102**. The analyte or biomarker sensor **1110** includes a counter electrode **1130***a*, a working electrode **1130***b* and a reference electrode **1130***c* wherein the analyte or biomarker. **1125** is sensed or detected on the working electrode **1130***b* by impedance cytometry that involves imposition of an alternating current to the counter electrode **1130***a* and working electrode **1130***b* in the presence of reference or ground electrode **1130***c*.

[0066] Microfluidic device **1101** illustrated in FIGS. **2**A, **2**B and **2**C is functionally independent of integrated cell-free fraction analysis and cell-rich fraction analysis microfluidic device **1000** illustrated in FIG. **1** but is functionally equivalent to the cell-free fraction analysis section **1100** of microfluidic device **1000** that includes analyte or biomarker sensor **1110** for detecting an analyte or biomarker in cell-free fraction **1102**, as described above with respect to FIG. **1**, with the exception that the cell-rich fraction **1202** that is skimmed from whole blood sample **104** is rejected at whole blood sample rejection outlet **1202'** while cell-free fraction **1102** is analyzed via the analyte or biomarker sensor **1110**. Whole blood sample **104** is introduced at whole blood sample inlet port **1112** via generally one micropump such as micropump **105** in FIG. **1**. The microfluidic device **1101** includes a plasma skimming module **1114**, illustrated in the example shown in FIGS. **2**A-**2**C, as a plurality of parallel channels according to one embodiment of the present disclosure, from which the cell-free fraction **1102** is directed as separated plasma **1116** through separated plasma channels **1116'** that intersect, in the example shown in FIGS. **2**A-**2**C orthogonally, the plasma skimming channels **1114**. The separated plasma **1116** is directed to flow through the separated plasma channels **1116'** toward analyte detection microfluidic channel or recess or chamber **1118** (see also FIG. **2**C) defined in upper or working surface **1120** where analyte or biomarker **1125** is electrochemically detected by analyte sensor **1110** that may be a 3-electrode electrochemical detector **1130** as shown (see also FIG. **2**B). Thus, the plasma skimming module **1114** is configured and disposed to separate plasma **1116** from the whole blood sample **104** prior to entry of the whole blood sample **104** into the detection chamber **1118**.

[0067] The 3-electrode electrochemical detector **1130** includes linear strip electrode **1130***a* having an arcuately shaped counter electrode tip **1130***a'*, linear strip electrode **1130***b* having an arcuately shaped reference electrode tip **1130***b'* and linear strip electrode **1130***c* having a circularly shaped working electrode tip **1130***c'* that is disposed in recess **1118** so that the counter electrode tip **1130***a'* and the reference electrode tip **1130***c'* are concentrically arranged around the working electrode tip **1130***b'*. The working electrode tip **1130***b'* may be modified with a redox cycling system (not shown) to amplify the electrochemical signal of the analyte or biomarker **1125** that is present in the whole blood sample **104**. Other systems or methods of amplifying the electrochemical signal may also be employed and a redox cycling system is one example. The linear strip electrodes **1130***a*, **1130***b* and **1130***c* form connections to external electronics, such as a potentiostat (not shown) for signal detection. Following signal detection by the electrochemical analyte detector **1110** for the presence of analyte or biomarker **1125**, the separated plasma **1116** is then drawn out through the separated plasma sample outlet port **1124** such as by application of a vacuum connection, not shown, at whole blood sample rejection outlet **1202'** and at separated plasma sample outlet port **1124** or other means known in the art, such as by application of positive pressure via the micropump **105** (see FIG. **1**) at whole blood sample inlet port **1112** as described above.

[0068] Referring to FIG. **1**, the cell-rich fraction analysis section **1200** of integrated microfluidic device **100** relies on impedance measurements to establish a differential white blood cell count. While parallel electrodes as utilized in the prior art offer advantages in terms of accuracy, they are a significant factor in fabrication complexity. By employing coplanar electrodes, device assembly is simplified at least by reducing the number of physical layers required from three to two. Flow channels are defined in polydimethylsiloxane (PDMS) fabricated by established molding techniques, thereby reducing complexity over the use of photolithographically patterned polyimide and micromilled polymethyl methylacrylate (PMMA). Thus, the microfluidic device **1000** for differential white blood cell counting enables low-cost, scalable fabrication.

[0069] The loss in performance by utilizing coplanar compared to parallel electrodes is about 20%, notably decreasing for increasing cell size [15]. To retain or exceed the performance over the prior art, channels with height matched to the size of the particle or cell of interest, and thus smaller equivalent aperture D_A, are employed [13]. The channel height is comparable to the white blood cell diameters at below 20 μm, thus also reducing the impact of vertical cell position in the flow on the measured signal [15]. Lateral constraint is provided not by the channel itself, but rather by sheath flow focusing using pure water. This phenomenon relies on laminar flow and, via at least one micropump (not shown) that is generally external to the microfluidic device **1000**. In the embodiments of the present disclosure, the micropump is employed to introduce lysis flow of deionized water to create a lysate stream and to cause flow focusing by introducing fluid streams of deionized water to either side of the sample stream to force central alignment of cells [16, 17].

[0070] The micropump **105** is employed to introduce the whole blood sample **104** into the blood separation section **1002**. The introduction of the lysis flow and of the focusing flows may be accomplished by either a single external pump or separate dedicated pumps, one for the lysis flow and one for the focusing flow or flows.

[0071] Providing a virtual non-conductive aperture limits the danger of channel clogging in contrast to physical channel confinement [7, 10]. While this hydrodynamic focusing effect is well-studied, and is applied in bench-top flow cytometers, application of the hydrodynamic focusing effect in a microfluidic device such as microfluidic device **1000** to enhance differential white blood cell detection performance in an impedance-based lab on a chip (LOC) device represents a novel means for differential white blood cell detection.

[0072] For differential white blood cell counting, the high background of red blood cells should be eliminated prior to the impedance cytometer. Rather than employing chemical reagents to eliminate erythrocyte interference, pure water is employed. For clinical application, limiting the amount of required chemicals is an important consideration, as additional reagents complicate LOC packaging. Exposure of the cell stream to pure water creates a strong osmotic gradient

across plasma membranes, causing swelling and ultimately lysis [18, 19]. White blood cells are much more resistant to osmotic gradients than red blood cells, with neutrophils surviving more than three times as long as erythrocytes [20]. Although the white blood cells also swell due to the osmotic gradient, they survive intact to a much larger degree than red blood cells, thereby enabling the detection process disclosed herein of impedance cytometry.

[0073] To accommodate osmotic lysis in the microfluidic device **1000**, streams of pure water are symmetrically introduced to the sample flow a certain distance prior to the impedance cytometry region. In conjunction with the operating characteristics of the whole blood sample micropump **105** and the dedicated lysis injection and flow focusing inject water micropump (not shown) as described above, the distance and flow speeds are tuned such that the osmotic stress exposure prior to measurement results in lysis of red, but not white, blood cells. The osmotic swelling experienced by the white blood cells (i.e., leukocytes) heterogeneously affects sub-populations to further enhance differences probed by impedance cytometry. Microfluidic device **1000** represents a novel application of pure water osmotic lysis in a white blood cell counter to enhance the signal-to-noise ratio.

[0074] A microfluidic device design incorporating the features described above is shown in FIG. **3**. More particularly, FIG. **3** illustrates a microfluidic device **1201** that is also physically independent of integrated cell-free fraction analysis and cell-rich fraction analysis microfluidic device **1000**, and is thus a standalone device with respect to microfluidic device **1000**, but which is functionally equivalent to the cell-rich fraction analysis section **1200** of microfluidic device **1000**. Therefore, microfluidic device **1201** includes cell pre-treatment sub-section **1210** and cellular analysis sub-section **1230** for establishing a differential white blood cell count in the lysate with intact white blood cells **1220**, as described above with respect to FIG. **1**, but with the exception that instead of separating the whole blood sample **104** from the patient or subject **102** into cell-free fraction **1102** and cell-rich fraction **1202**, the whole blood sample **104** is now pumped, via one or more micropumps such as the generally one micropump **105** that may be externally positioned with respect to the microfluidic device **1201**, as described above schematically in FIG. **1**, or embedded within the microfluidic device **1201** (not shown), directly into the inlet of whole blood receiving channel **104'**.

[0075] As defined herein, a microfluidic device according to embodiments of the present disclosure may receive a whole blood sample and separate the whole blood sample into a cell-free fraction and into a cell-rich fraction and subject both the cell-free fraction and the cell-rich fraction to electrically-based analysis techniques.

[0076] As defined herein, a microfluidic device according to embodiments of the present disclosure may receive a whole blood sample and separate the whole blood sample into a cell-free fraction and into a cell-rich fraction and subject the cell-rich fraction to a means for causing lysis on the cell-rich fraction to form a lysate stream with intact white blood cells.

[0077] As defined herein, a microfluidic device according to embodiments of the present disclosure may receive a whole blood sample and subject the whole blood sample to a means for causing lysis on the whole blood sample to form a lysate stream with intact white blood cells without having first separated the whole blood cells into a cell-free fraction and into a cell-rich fraction.

[0078] Additionally, as defined herein, a microfluidic device according to embodiments of the present disclosure may receive a whole blood sample and separate the whole blood sample into a cell-free fraction and into a cell-rich fraction and subject only the cell-free fraction to an electrically-based analysis technique or subject only the cell-rich fraction to an electrically-based analysis technique.

[0079] Accordingly, the method of testing also may include directing the cell-rich fraction **1202**, or, in the embodiment of the microfluidic device **1201** of FIG. **3**, directing the whole blood sample **104** to a cell pre-treatment sub-section **1210** of cell-rich analysis section **1200** wherein pre-treatment may include lysis of the whole blood sample **104**, directing the resulting lysate with intact white blood cells **1220** to a lysate analysis or impedance cytometry sub-section **1230** and directing impedance cytometry results **1240** as all or part of point-of-care information **106** provided by the microfluidic device **1000**.

[0080] Consequently, microfluidic device **1201** in FIG. **3** illustrates in more detail the cell-rich fraction analysis section **1200** of microfluidic device **1000** as formed in cell-rich fraction analysis section microfluidic layer **1201'** (for illustration purposes) as a whole blood sample analysis section **12001**. Microfluidic device **1201** includes sample flow channel **1040'** that is configured and disposed to receive a whole blood sample **1040** that is directed into the sample flow channel **1040'** and wherein a first lysis flow channel **1204*a'*** receives a first lysis flow **1204*a*** and a second lysis flow channel **1204*b'*** receives a second lysis flow **1204*b'*** such that the first lysis flow channel **1204*a'*** and the second lysis flow channel **1204*b'*** intersect on opposing sides the sample flow channel **1040'** in a quasi-tee or converging forked configuration **1205** to enable mixing of the sample flow **1040** with the first lysis flow **1204*a*** and with the second lysis flow **1204*b***. The first lysis flow **1204*a*** and the second lysis flow **1204*b*** may be of de-ionized water. The sample mixture **1206** is directed into pre-treatment section **1210** that includes a series of channel loops **1208*a*** . . . **1208*n***, that are sufficient in number and length to provide sufficient exposure duration time of the sample cells in the sample mixture **1206** to the de-ionized water to cause lysis of the erythrocyte cells such that the sample mixture **1206** emerges from the channel loops **1208*a*** . . . **1208*n*** as a lysate stream **1212** with intact white blood cells which are directed into a lysate channel **1212'**.

[0081] Thus, the lysate stream **1212** is directed into lysate flow channel **1212'** wherein a first focusing flow channel **1214*a'*** receives one or more focusing flows, e.g., a first focusing flow **1214*a*** and a second focusing flow channel **1214*b'*** receives a second focusing flow **1214*b'*** such that, in a similar manner as with respect to the lysis flow described above, the first focusing flow channel **1214*a'*** and the second focusing flow channel **1214*b'*** intersect on opposing sides the lysate flow channel **1212'** in a quasi-tee or forked configuration **1208** to enable the lysate stream **1212** to be directed into a lysate stream channel **1220'** that is configured and disposed in the microfluidic layer **1201'** such that a lysate stream **1212"** with intact white blood cells is directed to flow in a direction of motion, as indicated by arrow A, in the lysate stream channel **1220'**. At least two deionized water injection channels **1214*a'*** and **1214*b'*** are configured and disposed in the microfluidic device **1000** such that at least two streams of deionized water **1214*a*** and **1214*b*** are directed into the lysate stream channel **1220'** to force the lysate stream **1212"** to flow in the direction of motion A between two streams of deionized water **1214*a"***

and **1214***b*", respectively, to form a virtual non-conductive aperture **1222** in the lysate stream channel **1220**'.

[0082] In one embodiment, the one or more deionized water injection channels **1214***a*' and **1214***b*' are configured and disposed to symmetrically focus the two or more streams of deionized water **1214***a* and **1214***b* orthogonally on opposing sides of the direction of motion A of the lysate stream **1212**" in the lysate stream channel **1220**'.

[0083] The microfluidic device **1000** further includes an impedance cytometry section **1230** wherein at least two co-planar electrodes, e.g., electrodes **1230***a***1**, **1230***a***2** or **1230***b***1**, **1230***b***2** or **1230***c***1**, **1230***c***2** or **1230***d***1**, **1230***d***2**, are configured and disposed on a surface **1203** of the microfluidic layer **1201**' such that the white blood cells/leukocytes in the lysate stream channel **1220**' are exposed to an alternating current at at least one frequency emitted from the at least two co-planar electrodes **1230***a***1**, **1230***a***2** or **1230***b***1**, **1230***b***2** or **1230***c***1**, **1230***c***2** or **1230***d***1**, **1230***d***2**. The co-planar electrodes are configured in sequential sets of co-planar parallel electrode pairs **1230***a***1**, **1230***a***2** followed by **1230***b***1**, **1230***b***2** followed by **1230***c***1**, **1230***c***2** followed by **1230***d***1**, **1230***d***2** that are each positioned orthogonally on the surface **1201** such that the lysate stream channel **1220**' crosses over in an orthogonal manner each of the sequential sets of co-planar parallel electrode pairs.

[0084] Thus, the impedance measurements rely on sequential sets of parallel electrode pairs—one for low-frequency measurements, e.g., **1230***a***1** and **1230***a***2**, and one for high-frequency measurements, e.g., **1230***b***1** and **1230***b***2**. Two additional pairs of electrodes, e.g., **1230***c***1**, **1230***c***2** and **1230***d***1**, **1230***d***2**, are included as optional references at the respective frequencies to allow for differential measurements, assuming a cell density resulting in spacing between individual cells larger than the electrode gap (see FIGS. **5** and **6** as described below).

[0085] At a known flow rate, the sequential measurements can be correlated for each cell. Sample flow is provided by pressure actuation from external syringe pumps, e.g., one or more micropumps **105** as shown in FIG. **1**, connected through capillary tubing. External electronics for signal recording, connected to a microprocessor such as a personal computer (PC) running LabVIEW (National Instruments, Inc., Austin, Tex., USA), may be employed for data acquisition. The external electronics may include impedance recording equipment such as an impedance analyzer or LCR meter (e.g., IET/QuadTech 1910/1920 1 MHz LCR Meter, IET Labs, Inc., Roslyn Heights, N.Y., USA).

[0086] The presence of the sequential sets of co-planar parallel electrode pairs **1230***a***1**, **1230***a***2** followed by **1230***b***1**, **1230***b***2** followed by **1230***c***1**, **1230***c***2** followed by **1230***d***1**, **1230***d***2** enables performing impedance cytometry of the white blood cells/leukocytes in the lysate stream **1212**" in the lysate stream channel **1220**' at the one or more frequencies. For example, as illustrated in FIGS. **5** and **6** and described below, as an intact white blood cell traverses into the gap between each pair of electrodes, co-planar parallel electrode pair **1230***a***1**, **1230***a***2** and co-planar parallel electrode pair **1230***b***1**, **1230***b***2** may each be operated at, for example, 100 kilohertz (kHz) and (absolute values of) impedance measurements Z in ohms (Ω) or in percent change in (absolute values of) impedance ΔZ may be taken. These measurements may be repeated by co-planar parallel electrode pair **1230***c***1**, **1230***c***2** and co-planar parallel electrode pair **1230***d***1**, **1230***d***2** when the intact white blood cell traverses into the respective gap between each pair of electrodes.

[0087] Alternatively, as an intact white blood cell traverses into the gap between each pair of electrodes, co-planar parallel electrode pair **1230***a***1**, **1230***a***2** may be operated at, for example, 100 kilohertz (kHz) and co-planar parallel electrode pair **1230***b***1**, **1230***b***2** may be operated at, for example, 500 kilohertz (kHz) and (absolute values of) impedance measurements Z in ohms (Ω) or in percent change in (absolute values of) impedance ΔZ may be taken. These measurements may be repeated by co-planar parallel electrode pair **1230***c***1**, **1230***c***2** operating at 100 kHz and co-planar parallel electrode pair **1230***d***1**, **1230***d***2** operating at 500 kHz when the intact white blood cell traverses into the respective gap between each pair of electrodes.

[0088] The method includes quantitatively differentiating between neutrophils, lymphocytes, monocytes, eosinophils, and basophils in the lysate stream **1212**" based on impedance measurements resulting from the performance of the impedance cytometry as described above.

[0089] Upon flow of the lysate stream **1212**" in the lysate stream channel **1220**' across the sequential sets of co-planar parallel electrode pairs **1230***a***1**, **1230***a***2** followed by **1230***b***1**, **1230***b***2** followed by **1230***c***1**, **1230***c***2** followed by **1230***d***1**, **1230***d***2**, the lysate stream **1212**" is directed to a waste flow outlet **1224**.

[0090] FIG. **4** illustrates an alternate embodiment of microfluidic device **1201** described above with respect to FIG. **3**, and is thus another example of a standalone device with respect to microfluidic device **1000** in FIG. **1**. Microfluidic device **1251** illustrates in more detail the cell-rich fraction analysis section **1200** of microfluidic device **1000** as formed in microfluidic layer **1251**' (for illustration purposes) as a whole blood sample analysis section **12002**. More particularly, whole blood sample analysis section **12002** is identical to whole blood sample analysis section **12001** in FIG. **3** except that whole blood sample analysis section **12002** includes a common water lysis flow inlet **1204** for the first lysis flow channel **1204***a*' that receives first lysis flow **1204***a* and for the second lysis flow channel **1204***b*' that receives second lysis flow **1204***b'*.

[0091] Similarly, whole blood sample analysis section **12002** includes a common water focus flow inlet **1214** for the first focusing flow channel **1214***a*' that receives first focusing flow **1214***a* and for the second focusing flow channel **1214***b*' that receives second focusing flow **1214***b'*.

[0092] Additionally, whole blood sample analysis section **12002** formed in microfluidic layer **1251**' further includes the sequential sets of co-planar parallel electrode pairs **1230***a***1**, **1230***a***2** followed by **1230***b***1**, **1230***b***2** followed by **1230***c***1**, **1230***c***2** followed by **1230***d***1**, **1230***d***2** that are respectively connected to a power supply and impedance recording equipment (not shown), such as an impedance analyzer or LCR meter, (e.g., IET/QuadTech 1910/1920 1 MHz LCR Meter, IET Labs, Inc., Roslyn Heights, N.Y., USA) via connections and pads **1230***a***10** and **1230***a***20** for electrodes **1230***a***1** and **1230***a***2**, respectively, connections and pads **1230***b***10** and **1230***b***20** for electrodes **1230***b***1** and **1230***b***2**, respectively, connections and pads **1230***c***10** and **1230***c***20** for electrodes **1230***c***1** and **1230***c***2**, respectively, and connections and pads **1230***d***10** and **1230***d***20** for electrodes **1230***d***1** and **1230***d***2**, respectively. Although not obvious from FIG. **4** due to the microscopic scale of the electrodes and channels, the electrodes **1230***a***1**, **1230***a***2**, **1230***b***1**, **1230***b***2**, **1230***c***1**, **1230***c***2**, **1230***d***1**, **1230***d***2** are positioned under lysate stream **1220** in the same sequential manner as displayed in FIG. **3**. The con-

nection pads **1230***a***1**, **1230***b***1**, **1230***c***1** and **1230***d***1** are disposed on the left side of lysate stream **1212"** with respect to the downstream direction of flow while connection pads **1230***a***2**, **1230***b***2**, **1230***c***2** and **1230***d***2** are disposed on the right side of lysate stream **1212"** with respect to the downstream direction of flow.

[0093] Again, the impedance measurements rely on sequential sets of parallel electrode pairs—one for low-frequency and one for high-frequency measurements. Two additional pairs of electrodes are included as optional references at the respective frequencies to allow for differential measurements, assuming a cell density resulting in spacing between individual cells larger than the electrode gap. At a known flow rate, the sequential measurements can be correlated for each cell. Sample flow is provided by pressure actuation from external syringe pumps, connected through capillary tubing. External electronics are utilized for signal recording, connected to a PC running LabVIEW for data acquisition.

[0094] The lysate stream **1212"** with intact white blood cells is directed to flow in the direction of motion, as indicated by arrow A, in the lysate stream channel **1220'**. At least two streams of deionized water **1214***a* and **1214***b* are directed into the lysate stream channel **1220'** such that the lysate stream **1212"** is forced to flow in the direction of motion A between two streams of deionized water **1214***a***"** and **1214***b***"**, respectively, to form the virtual non-conductive aperture **1222** in the lysate stream channel **1220'**.

[0095] It should be noted that although the foregoing and subsequent description of microfluidic devices **1201** in FIGS. **3** and **1251** in FIG. **4** is presented as representative examples of the lysis sub-section **1210** to form lysate stream **1212** and of the lysate analysis section **1230** that enables analysis of the compressed lysate stream **1212"** from the cell-rich fraction **1202**, the integrated microfluidic device **1000** need not be limited to detection of white blood cells but may also be applied to cytometry of other cells such as the known various sub-types of white blood cells and circulating tumor cells and except for red blood cells since the lysis is intended to remove such cells from the lysate stream **1212**, Other methods cell detection for the integrated device **1000** may include visual or optical detection via observation of the lysate stream **1212** under a microscope.

[0096] Fabrication & Instrumentation

[0097] Gold coplanar electrodes were photolithographically patterned on a glass or silicon oxide substrate as one example, and SU-8 photoresist was used to create a negative master structure on silicon. Positive PDMS microfluidics can thus be molded and cured, and subsequently bonded to the glass reversibly by simple application of pressure, or permanently by prior application of oxygen plasma and thus fabricated by standard microfabrication approaches. Gold could conceivably also be another chemically inert conductor. As described above, the impedance measurements rely on the sequential sets of parallel electrode pairs—one for low-frequency and one for high-frequency measurements. Two additional pairs of electrodes are included as optional references at the respective frequencies to allow for differential measurements, assuming a cell density resulting in spacing between individual cells larger than the electrode gap. At a known flow rate, the sequential measurements can be correlated for each cell. Sample flow is provided by pressure actuation from external syringe pumps, connected through capillary tubing. Again, external electronics for signal recording, such as a potentiostat, impedance analyzer, or LCR meter as described above are connected to a PC running LabVIEW for data acquisition.

[0098] For the microfluidic layer, a mold was created using SU-8 2015 negative photoresist patterned on silicon using contact photolithography. Using this master, channels were cast from poly(dimethylsiloxane) (PDMS). After thermal curing at 60° C., the PDMS was diced and 2 mm diameter fluidic connections were punched.

[0099] Referring to FIGS. **5** and **6**, thus the microfluidic devices **1201** and **1251** illustrated in FIGS. **3** and **4**, respectively, and as further described below with respect to microfluidic device **1000** in FIGS. **12**, **12**A and **12**B, comprise two physical layers. Four pairs of microelectrodes **1230***a***1**, for impedance measurements **1230***a***1**, **1230***a***2** followed by **1230***b***1**, **1230***b***2** followed by **1230***c***1**, **1230***c***2** followed by **1230***d***1**, **1230***d***2** each have a width dimension We with gap G between the two electrodes in each pair and are disposed on a lower or first layer of glass or silicon oxide layer via a chrome adhesive therebetween. In one embodiment, the width We is about 25 μm and the gap G is also about 25 μm. The microfluidic channels are formed in an upper or second layer of PDMS wherein the microfluidic channels are formed with a cross-section of 75×20 μm2 (width×height). The lysate stream channel **1220'** has a channel width W of about 75 μm and a height H of about 20 μm. The upper or second layer of PDMS is formed on both the electrodes and the lower or first layer substrate of glass or silicon oxide. The PDMS is plasma-bonded to the glass and also seals and adheres to the gold coplanar electrodes.

[0100] FIG. **5** illustrates one embodiment of a portion of the whole blood analysis section **1200** of microfluidic device **1201** as illustrated in FIG. **3** and microfluidic device **1251** as illustrated in FIG. **4**. Water focusing flows **1214***a* and **1214***b* are directed into the lysate stream **1212** in lysate channel **1212'**. Lysate channel **1212'** intersects between first focusing flow channel **1214***a***'** and second focusing flow channel **1214***b***'** in a crossed intersection **1205** such that when the two or more streams of deionized water **1214***a* and **1214***b* are directed into the lysate stream channel **1220'**, a compressed lysate stream **1212"** is forced to flow in the direction of motion A between two streams of deionized water **1214***a***"** and **1214***b***"**, respectively, to form virtual non-conductive aperture **1222** in the lysate stream channel **1220'**.

[0101] The lysate stream channel **1220'** is positioned over sequential sets of co-planar parallel electrode pairs **1230***a***1**, **1230***a***2** followed by **1230***b***1**, **1230***b***2** such that a detection region **1231** for white blood cells is formed by the gap G between the set of co-planar parallel electrode pairs **1230***a***1**, **1230***a***2** and by the gap G between the set of co-planar parallel electrode pairs **1230***b***1**, **1230***b***2**. Detection of white blood cells occurs by electric fields from the sequential sets of co-planar parallel electrode pairs **1230***a***1**, **1230***a***2** and **1230***b***1**, **1230***b***2** propagating through the virtual aperture **1222** in the gaps G.

[0102] Referring also to FIG. **6**, in one embodiment, the presence of the sequential sets of co-planar parallel electrode pairs **1230***a***1**, **1230***a***2** followed by **1230***b***1**, **1230***b***2** followed by **1230***c***1**, **1230***c***2** followed by **1230***d***1**, **1230***d***2** enables performing impedance cytometry of the white blood cells/leukocytes in the lysate stream **1212"** in the lysate stream channel **1220'** at the one or more frequencies. For example, as an intact white blood cell **12120** traverses into the gap G between each pair of electrodes, co-planar parallel electrode

pair **1230***a***1**, **1230***a***2** and co-planar parallel electrode pair **1230***b***1**, **1230***b***2** may each be operated at, for example, 100 kilohertz (kHz) and (absolute values of) impedance measurements Z in ohms (Ω) or in percent change in (absolute values of) impedance ΔZ may be taken. These measurements may be repeated by co-planar parallel electrode pair **1230***c***1**, **1230***c***2** and co-planar parallel electrode pair **1230***d***1**, **1230***d***2** when the intact white blood cell **12120** traverses into the respective gap G between each of those pairs of electrodes.

[0103] In still another embodiment, as an intact white blood cell **12120** traverses into the gap G between each pair of electrodes, co-planar parallel electrode pair **1230***a***1**, **1230***a***2** may be operated at, for example, 100 kilohertz (kHz) and co-planar parallel electrode pair **1230***b***1**, **1230***b***2** may be operated at, for example, 500 kilohertz (kHz) and (absolute values of) impedance measurements Z in ohms (Ω) or in percent change in (absolute values of) impedance ΔZ may be taken. These measurements may be repeated by co-planar parallel electrode pair **1230***c***1**, **1230***c***2** operating at 100 kHz and co-planar parallel electrode pair **1230***d***1**, **1230***d***2** operating at 500 kHz when the intact white blood cell traverses into the respective gap between each pair of electrodes. It is assumed that each electrode pair operates at one specific frequency, but as the intact white blood cell **12120** travels through lysate stream channel **1220'** the cell will experience the particular operating frequency of each pair of electrodes.

[0104] For both of the foregoing methods of measuring changes in impedance, the measurements at the coplanar electrode pair **1230***b***1**, **1230***b***2** and at coplanar electrode pair **1230***d***1**, **1230***d***2** are considered to be "empty channel" readings since the microfluidic devices **1201** and **1251** should be designed such that statistically it is anticipated that while an intact white blood cell **12120** traverses into the gap G between electrode pair **1230***a***1**, **1230***a***2**, or between electrode pair **1230***c***1**, **1230***c***2**, no particle is anticipated to be present in the gap G between electrode pair **1230***b***1**, **1230***b***2** or electrode pair **1230***d***1**, **1230***d***2**, respectively while the impedance measurements are being recorded.

[0105] Modeling

[0106] Extensive use of finite element modeling (FEM) was made, in combination with equivalent circuit modeling, to guide the design process, as described below. Critical parameters such as channel cross-section and electrode gap were chosen based on model optimization. Finite element modeling (FEM) was performed in COMSOL Multiphysics (COMSOL, Inc.; Palo Alto, Calif.), using the MEMS and Microfluidics packages.

[0107] The 2D (two-dimensional) hydrodynamic model considered a slow-diffusing species (particles) and a fast-diffusing species (ions) introduced through a center sample channel, focused symmetrically by deionized water (DI-H2O) flows.

[0108] A representative simulation is shown in FIG. **5**. The main model outputs of interest are the cross-sectional concentration profiles downstream from the flow focusing inlets—the respective full width at half maximum (FWHM) for the ions can be considered equivalent to the VA width. The smaller the dimension of the virtual aperture VA, and thus the dimension of FWHM, the greater the accuracy of the impedance measurements since the impedance measurements mainly only reflect the intact white blood cell **12120** in contrast to the impedance of the two streams of deionized water **1214***a***"** and **1214***b***"**. As an additional means of increasing accuracy of the impedance measurements, the distance X between the convergent tee **1208** and the upstream edge **1230***a***1'** of the first electrode **1230***a***1** is also designed to a minimum value so that the impedance measurements occur at a position before significant divergence of the virtual aperture VA occurs downstream of the final electrode **1230***d***2**. The spacing between the coplanar electrodes **1230***a***1**, **1230***a***2** followed by **1230***b***1**, **1230***b***2** followed by **1230***c***1**, **1230***c***2** followed by **1230***d***1**, **1230***d***2** generally does not significantly affect the impedance measurements as long as the electrodes are located before any significant divergence of the virtual aperture VA occurs.

[0109] FIG. **6** illustrates a perspective sample model geometry which represents the detection portion **1231** identified in FIG. **5**. The model output is the change in impedance |ΔZ| measured across electrodes between particle and no-particle conditions.

[0110] Referring also to FIG. **5**, the 3D electrodynamic model simulates particle **12120** of the lysate stream **1212"** having radius r, conductivity a, and permittivity e, suspended in a section of microfluidic channel, i.e., lysate stream channel **1220'** which defines first vertical channel wall **1226***a* and second vertical channel wall **1226***b*, in the gap G between two coplanar electrodes, e.g., electrodes **1230***a***1** and **1230***a***2**. To approximate the impact of hydrodynamic focusing, two distinct environments (apart from the particle) were incorporated within the segment of lysate stream channel **1220'**—electrolyte (compressed lysate stream **1212"**) in the center at a certain width Wp corresponding to VA, and deionized water focus flows **1214***a* and **1214***b* on opposing sides of the compressed lysate stream **1212"**. The deionized water focus flows **1214***a* and **1214***b* define respectively deionized water focus flow width W_{H20}a between channel wall **1226***a* and the compressed lysate stream **1212"** and deionized water focus flow width W_{H20}b between channel wall **1226***b* on the opposite side of the compressed lysate stream **1212"** and of the lysate stream channel **1220'**. As indicated above, the model output is the change in impedance |ΔZ| measured across electrodes between particle and no-particle conditions.

[0111] Thus the virtual aperture VA represents the cross-sectional area defined by the width W and height H of the lysate stream **1212"**, excluding the widths W_{H2Oa} and W_{H2Ob} of the deionized water focus flows **1214***a* and **1214***b* in the channel **1220'**.

[0112] It should also be noted that although the microfluidic devices **1000**, **1201** and **1251** are described and illustrated in FIGS. **1-6** and later in FIGS. **12**, **12**A, **12**B below as configured to receive two deionized water lysis flows **1204***a* and **1204***b*, only one lysis flow such as **1204***a* or **1204***b* is required, or the microfluidic devices **1000**, **1201** and **1251** may be configured to receive additional lysis flow or flows (not shown).

[0113] Additionally, although the microfluidic devices **1000**, **1201** and **1251** are described and illustrated in FIGS. **1-6** and later in FIGS. **12**, **12**A, **12**B below as configured to receive two deionized water focus flows **1214***a* and **1214***b*, only one focus flow such as **1214***a* or **1214***b* is required, in which case the virtual aperture VA occurs directly between second vertical channel wall **1226***b* and focus flow **1214***a* or between first vertical channel wall **1226***a* and focus flow **1214***b*.

[0114] Alternatively, the microfluidic devices **1000**, **1201** and **1251** may be configured to receive additional focus flow or flows (not shown).

[0115] Experiments

[0116] The fabricated microfluidic devices were connected to syringes using Tygon tubing (Cole-Parmer; Vernon Hills, Ill., USA). Constant flow was provided through syringe pumps (KDS230 (KD Scientific, Inc.; Holliston, Mass., USA), Genie Plus (Kent Scientific Corporation; Torrington, Conn., USA), NE-300 (New Era Pump Systems, Inc.; Farmingdale, N.Y., USA)). Admittance measurements for model verification were done using a VSP-300 potentiostat (Bio-Logic; Claix, France).

[0117] Impedance cytometry data was recorded via LabView utilizing an E4980A Precision LCR Meter (Agilent; Santa Clara, Calif., USA). The background signal was determined through MATLAB (MathWorks, Inc.; Natick, Mass., USA) robust local regression smoothing of the raw data, the signal peaks using a peak finding algorithm. Population averages were calculated using histogram peak fits in OriginPro (OriginLab Corporation; Northampton, Mass., USA).

[0118] Prior to use, the LOCs were rinsed with Fetal Bovine Serum (FBS; Life Technologies; Carlsbad, Calif., USA) to reduce PDMS hydrophobicity. Polystyrene particles (r=3 μm and 5 μm; sulfate-type) were purchased from Life Technologies (Carlsbad, Calif., USA) and suspended in phosphate-buffered saline (PBS; 1× from tablet; Sigma-Aldrich; St. Louis, Mo., USA). To reduce settling velocity through density matching, sucrose (Sigma-Aldrich; St. Louis, Mo., USA) was added to 14% w/v. All solutions were based on DI-H2O (ρ=18 Ωcm).

[0119] It should be noted that although the impedance cytometry measurements are generally recorded via application of alternating current (AC), it is possible to record impedance cytometry measurements via direct current (DC) although generally the signal-to-noise ratio is reduced as compared to the AC measurements. In the case of DC impedance cytometry, the impedance measurements are a static measurement of resistance R based on R=V/I with respect to time, where V is the applied voltage and I is the measured current.

[0120] Results and Discussion

[0121] Hydrodynamic Model and Validation

[0122] Referring to FIG. **7**, the flow rates are the main external parameters to control the VA width, the critical parameter for impedance cytometry performance. To elucidate their correlation, hydrodynamic FEM was utilized to determine the ionic FWHM for a range of flow ratios (FR) of phosphate-buffered saline (PBS)-based sample to DI-H2O focus. In FIG. **7**, the left vertical axis is virtual aperture width VA (or Wp) in microns (μm) plotted against horizontal axis of flow ratio sample to focus FR (1:x) where the FEM results are indicated in circles and the experimental results are indicated by crosses. The results are in qualitative agreement with theory [7]. As expected intuitively, the virtual aperture width VA (or Wp) decreases drastically over 80 microns at zero FR to approximately 3-4 microns as flow focusing is introduced, with the effect saturating at high flow ratios. The behavior is independent of flow rate, at least in the laminar flow regime.

[0123] To verify these results in the experimental microfluidic device that was utilized, a pure PBS sample flow (10, 20, 50, 100 μl/h) and DI-H2O focus flows (100 μl/h combined) were introduced. To achieve FR=0, PBS was substituted for the deionized water DI-H2O. The left vertical axis is fluid admittance at 200 kHz in microsiemens (μS). The admittance of the fluid across electrodes, which at 200 kHz is dominated by ionic conduction, was measured. Thus, this parameter is expected to linearly correlate with the ionic FWHM. Indeed, the overlaid experimental data as represented by crosses in FIG. **7** aligns well with experimental model results as represented by circles, wherein the fluid admittance exceeds 35 μS at zero FR and decreases to about 5 μS at FR equal to approximately 17.5. The fact that the measured trend is toward a non-zero value at high FR can be attributed to parasitic currents in the real-world instrument-microfluidic device circuit.

[0124] Electrodynamic Model

[0125] To illustrate the advantages of hydrodynamic focusing in impedance cytometry, electrodynamic FEM is relied upon although analytical modelling may also be employed. In FIG. **8**, the vertical axis is the absolute value of the change in impedance |ΔZ| at 200 kHz as a percentage with respect to the empty channel impedance Z plotted against the horizontal axis of virtual aperture width in microns (μm). The cell radius R is 50 μm and the results are plotted for a 25 μm channel width (crosses) and for a 50 μm channel width (boxes) The relative |ΔZ| (i.e., as a percentage of the empty-channel Z) induced by an r=5 μm particle for a range of VA (or Wp widths is displayed. A frequency of f=200 kHz was found to be most sensitive to resistive properties, and thus r, and this was used throughout this work. The plot shows data for channel widths of 25 μm and 50 μm, revealing the signal is independent of the actual channel width (memory constraints prevented simulations for 75 μm width). Therefore, at the chosen f, the VA is expected to function in a manner identical to a physical constriction. As expected, the relative |ΔZ| induced by an r=5 μm particle increases significantly with decreasing VA. Specifically, reducing the aperture from 50 μm to 5 μm enhances the signal 10-fold from |ΔZ|=1.8% to |ΔZ|=18%. At very low VA≤r, the signal saturates, which can be attributed to the fact that in this regime, only part of the particle is in electrolyte and thus contributing to the signal. It is expected that in reality, a boundary layer of PBS would surround the particle, which would alter the results. However, considering the underlying approximation of a well-defined boundary between PBS and DI-H2O in this model, the additional error introduced by the omitted particle boundary layer is likely negligible.

[0126] Model Predictions:

[0127] Electrodynamic finite element modeling (FEM) effectively illustrates the expected utility of flow focusing in impedance cytometry. The relative ΔZ at 200 kHz induced by an R=5 μm cell, plotted in FIG. **9**, is increased up to 10-fold through flow focusing, and independent of the actual channel width.

[0128] The signal dependence on different cell parameters is illustrated in FIG. **9** which is a plot of FEM simulation of |ΔZ| for a cell with given r, $\in_{mem}$, and σ_{cyt} (solid black), where R=5 μm; $\in_{mem}=11.3\ \in_0$; $\sigma_{cyt}=0.6$ S/m (siemens/meter) versus frequency in Hz (plot **90**).

[0129] As compared to the plot **90**, low frequencies up to around 50 kHz, region **901**, are most sensitive to cell size, i.e., cell radius R=3.5 μm (plot **91**) and radius R=6.5 μm (plot **92**), while higher frequencies around 500 kHz, region **902**, respond to changes in membrane capacitance $\in_{mem}$ where $\in_{mem}$ is the cell permittivity of the cellular membrane, $\in_0$ is permittivity of the vacuum for $\in_{mem}=5.65\ \in_0$ (plot **93**) and $\in_{mem}=22.6\ \in_0$ (plot **94**), and to cytoplasm conductivity σ_{cyt} where $\sigma_{cyt}=0.3$ S/m (siemens/meter) (plot **95**) and $\sigma_{cyt}=1.2$ S/m) (plot **96**) around 5 MHz, region **903**.

[0130] This allows for the critical blood cell type differentiation based on multi-frequency measurements. The observed impact of cell size on the entire frequency range can be corrected for by considering impedance ratios, such as $\Delta Z_{500\ kHz}/\Delta Z_{50\ kHz}$ [15]. Preliminary consideration of the ionic double-layer by coupling FEM to a circuit model predicts an overall upward shift of those frequencies of highest sensitivity.

[0131] Preliminary Experiments

[0132] Preliminary experiments were conducted with polystyrene beads of sizes r=3 μm and 5 μm suspended in buffer solutions in a prototype device incorporating impedance cytometry and flow focusing, as partially depicted in FIGS. **5** and **6** as described above. The prototype device served to validate FEM results, and further to study the interplay of flow focusing and impedance cytometry.

[0133] While hydrodynamic focusing has been utilized to enhance the performance of coulter counter-type devices, no systematic study has been conducted on how flow ratios and geometry affect particle sizing sensitivity. Although FEM can give valuable insights into potential trends, these approximations are unlikely to capture the entirety of the system coupling.

[0134] FIG. **10** illustrates the impedance-based particle counting principle using the prototype device of FIGS. **5** and **6** with a mixture of both r=3 μm and 5 μm bead populations at a sample flow of 45 μl/h without flow focusing. The MATLAB-processed data shows distinct peaks in impedance |ΔZ| at 200 kHz in ohms (Ω) corresponding to particles passing between the electrodes as a function of time in seconds (s). Furthermore, three distinct populations become apparent, corresponding in order of increasing signal to 3 μm beads (|ΔZ|=94±9Ω), clusters of two 3 μm beads (|ΔZ|=162±23Ω) passing through gap G, and 5 μm beads (|ΔZ|=329±29Ω). While clusters of three or four 3 μm beads are statistically unlikely, their mis-identification as a 5 μm bead cannot be ruled out in this data due to their similar volume. Although the 3 μm bead population signal is well-defined, we note a larger spread in the cluster signals, which is in line with their non-spherical shape—based on orientation relative to the electrodes, the signal magnitude is expected to vary, as the electric field is not isotropic. This may enable more definitive differentiation between clusters of small particles and larger single particles through analysis of the transient signal during passage between the electrodes. The background is random noise from the environment etc.

[0135] To determine the impact of hydrodynamic focusing on sensitivity of the device, single-population samples of beads may be utilized, and the ratio of focus flow to sample flow (FR) may be varied while keeping the total flow rate (sample+focus) constant at 45 μl/h. From histograms based on data analogous to that shown in FIG. **10**, FIG. **11** is a plot of the average impedance |ΔZ| at 200 kHz in percent (%) for separate bead populations as a function of flow ratio sample to focus FR. The graph indicates up to 276% enhanced size-based differentiation, from Δ |ΔZ|=0.55% to Δ |ΔZ|=1.52%. Underlying this are overall increases in |ΔZ| by 277% and 275% for 3 μm and 5 μm beads, respectively. These numbers highlight the improved sensitivity enabled through the presently disclosed approach.

[0136] While the trend agrees with modeling in FIG. **9**, the magnitudes are lower than predicted. Specifically, at FR=1:7, modeling predicts VA≈8 μm in FIG. **7**, and in consequence |ΔZ|≈15% for r=5 μm beads in FIG. **8**. This almost order-of-magnitude difference compared to experimental results warrants further investigation. One potential explanation is the aforementioned model assumption of well-defined boundaries between PBS and DI-H2O in the electrodynamic FEM. However, this is unlikely to be solely responsible for the discrepancy.

[0137] Experimental causes such as parasitic capacitances, which become more dominant at high absolute Z (correlating with higher FR), will need to be explored.

[0138] Overall, separation efficiency increases with FR; at the same time, the sample throughput (equaling sample input flow rate) in the experimental results decreases (as total flow is kept constant). However, the sample flow rate is inherently independent from FR. In the laminar flow regime, sensitivity and throughput are thus decoupled in the LOC or microfluidic devices according to the present disclosure, enabling tailoring of these parameters to the specific experimental needs.

[0139] FIG. **12** illustrates a perspective view of one embodiment of the integrated microfluidic device **1000** that has been described schematically with respect to FIG. **1** above. More particularly, integrated microfluidic device **1000** includes whole blood sample inlet port **104'** wherein the whole blood sample **104** from the patient or subject **102** is directed to blood separation section **1002** of microfluidic device **1000**.

[0140] The integrated microfluidic device **1000** includes an upper layer or microfluidic layer of material **1232** that incorporates cell-rich fraction analysis section microfluidic layer **1201'** described above with respect to FIG. **3**.

[0141] Whole blood sample separation section **1002** is configured and disposed in the microfluidic layer of material **1232** to receive the sample **104** of whole blood of a subject via the whole blood sample inlet port **104'** and to separate the whole blood sample **104** into cell-free fraction **1102** and into cell-rich fraction **1202**.

[0142] In a similar manner as described above with respect to FIGS. **2**A, **2**B, **2**C described above, analyte sensor sub-section **1110** is configured and disposed in the microfluidic layer of material **1232** to detect an analyte **1125** in the cell-free fraction **1100**.

[0143] The analyte sensor sub-section **1110** includes counter electrode **1130***a*, a working electrode **1130***b* and a reference electrode **1130***c* wherein the analyte or biomarker **1125** is sensed or detected on the working electrode **1130***b* by impedance cytometry that involves imposition of an alternating current to the counter electrode **1130***a* and working electrode **1130***b* in the presence of reference or ground electrode **1130***c*. As described above with respect to FIGS. **1** and **2**, again, the analyte or biomarker **1125** may include, e.g, a drug or pharmaceutical, metabolites, vitamins, viruses, bacteria, hormones, enzymes, inflammatory mediators, chemokines, immunoglobulin isotypes, intracellular signaling molecules; apoptotic mediators; adhesion molecules, and antibodies etc.

[0144] The microfluidic device **1000** includes, as previously described above with respect to FIGS. **1** and **3-6**, the lysis sub-section **1210** that is configured and disposed on the microfluidic layer of material **1232** to form lysate stream **1212** from the cell-rich fraction **1202**, and also includes the lysate analysis section **1230** that is configured and disposed on the substrate **1010** to enable analysis of the compressed lysate stream **1212"** from the cell-rich fraction **1202**.

[0145] FIGS. **12**A and **12**B are cross-sectional views of the microfluidic device **1000** taken along section line **12**A-**12**A and section line **12**B-**12**B, respectively, wherein the upper

layer or microfluidic layer of material **1232** may be fabricated from PDMS or other suitable materials such as moldable plastic. All of the previously described features of the integrated microfluidic device **1000** of FIGS. **1** and **12**, or of the microfluidic device **1101** of FIGS. **2**A, **2**B, **2**C, or of the microfluidic device **1201** of FIG. **3** or microfluidic device **1251** of FIG. **4** and as further described in FIGS. **5** and **6** may be fabricated as described above for microfluidic device **1000**.

[0146] The co-planar electrodes **1130***a*, **1130***b*, **1130***c* and the co-planar electrodes **1230***a***1**, **1230***a***2**, **1230***b***1**, **1230***b***2**, **1230***c***1**, **1230***c***2**, **1230***d***1**, **1230***d***2** are disposed on a glass substrate **1236** via a chrome adhesive **1234** applied between the lower surfaces of the co-planar electrodes and the upper surface **1236'** of the glass substrate **1236**. The microfluidic device **1000**, and correspondingly microfluidic devices **1101**, **1201** and **1251**, is thus a composite **1010** of the glass substrate **1236** and the microfluidic layer **1232** including the coplanar electrodes **1130** for microfluidic device **1101** or coplanar electrodes **1230***a***1**, **1230***a***2**, **1230***b***1**, **1230***b***2**, **1230***c***1**, **1230***c***2**, **1230***d***1**, **1230***d***2** and connection pads **1230***a***10**, **1230***a***20**, **1230***b***10**, **1230***b***20**, **1230***c***10**, **1230***c***20**, **1230***d***10**, **1230***d***20** for microfluidic devices **1201** and **1251**, as appropriate, and the chrome adhesive layer **1234**.

[0147] Those skilled in the art will recognize and understand that the design and usage of the microfluidic devices **1000**, **1201** or **1251** are based upon calibration of the particular device to known cell types that have been verified to be present in the lysate stream **1212** via standard laboratory techniques.

[0148] As can be appreciated from the foregoing, the embodiments of the impedance-based microdevices described herein for differential white blood cell counts present at least the following novel features:

[0149] Reagent- and label-free assay (only water).

[0150] Integration of pure water hydrodynamic focusing to enhance signal-to-noise ratio.

[0151] Integration of pure water erythrocyte lysis to eliminate background signal and enhance white blood cell differentiation.

[0152] Two-layer design with PDMS channels and coplanar gold electrodes on glass for simple, low-cost fabrication.

[0153] Although the present disclosure has been described in considerable detail with reference to certain preferred version thereof, other versions are possible and contemplated. Therefore, the spirit and scope of the appended claims should not be limited to the description of the preferred versions contained therein.

[0154] While several embodiments of the present disclosure have been shown in the drawings, it is not intended that the disclosure be limited thereto, as it is intended that the disclosure be as broad in scope as the art will allow and that the specification be read likewise. Therefore, the above description should not be construed as limiting, but merely as exemplifications of particular embodiments. Those skilled in the art will envision other modifications within the scope of the claims appended hereto.

LIST OF REFERENCES

[0155] [1] K. Kottke-Marchant and B. Davis, *Laboratory Hematology Practice* (John Wiley & Sons, 2012).

[0156] [2] H. Craighead, Nature 442, 387 (2006).

[0157] [3] L. Rao, B. A. Ekberg, D. Connor, F. Jakubiak, G. M. Vallaro, and M. Snyder, Clinica Chimica Acta 389, 120 (2008).

[0158] [4] J. Nielsen, D. Thode, E. Stenager, K. Ø. Andersen, U. Sondrup, T. N.

[0159] Hansen, A. M. Munk, S. Lykkegaard, A. Gosvig, I. Petrov, and P. le Quach, European Neuropsychopharmacology 22, 401 (2012).

[0160] [5] H. Andersson and A. van den Berg, Sensors and Actuators B: Chemical 92, 315 (2003).

[0161] [6] D. A. Ateya, J. S. Erickson, P. B. H. Jr, L. R. Hilliard, J. P. Golden, and F. S. Ligler, Analytical and Bioanalytical Chemistry 391, 1485 (2008).

[0162] [7] K. C. Cheung, M. Di Berardino, G. Schade-Kampmann, M. Hebeisen, A. Pierzchalski, J. Bocsi, A. Mittag, and A. Tárnok, Cytometry Part A 77A, 648 (2010).

[0163] [8] H. Morgan, T. Sun, D. Holmes, S. Gawad, and N. G. Green, Journal of Physics D: Applied Physics 40, 61 (2007).

[0164] [9] M. E. Piyasena and S. W. Graves, Lab on a Chip (2014), 10.1039/c3lc51152a.

[0165] [10] T. Sun and H. Morgan, Microfluidics and Nanofluidics 8, 423 (2010).

[0166] [11] H. Zhang, C. H. Chon, X. Pan, and D. Li, Microfluidics and Nanofluidics 7, 739 (2009).

[0167] [12] D. Holmes, D. Pettigrew, C. H. Reccius, J. D. Gwyer, C. van Berkel, J. Holloway, D. E. Davies, and H. Morgan, Lab on a Chip 9, 2881 (2009).

[0168] [13] X. Han, C. van Berkel, J. Gwyer, L. Capretto, and H. Morgan, Analytical Chemistry 84, 1070 (2012).

[0169] [14] D. Holmes, J. K. She, P. L. Roach, and H. Morgan, Lab on a Chip 7, 1048 (2007).

[0170] [15] S. Gawad, L. Schild, and P. Renaud, Lab on a Chip 1, 76 (2001).

[0171] [16] X. Xuan, J. Zhu, and C. Church, Microfluidics and Nanofluidics 9, 1 (2010).

[0172] [17] G.-B. Lee, C.-C. Chang, S.-B. Huang, and R.-J. Yang, Journal of Micromechanics and Microengineering 16, 1024 (2006).

[0173] [18] J. Wessels, D. Pals, and J. Veerkamp, Biochimica et Biophysica Acta (BBA)—Biomembranes 291, 165 (1973).

[0174] [19] Y. Zhan, D. N. Loufakis, N. Bao, and C. Lu, Lab on a Chip 12, 5063 (2012).

[0175] [20] H. P. Ting-Beall, D. Needham, and R. M. Hochmuth, Blood 81, 2774 (1993).

[0176] [21] M. Evander, A. J. Ricco, J. Morser, G. T. Kovacs, L. L. Leung, L. Giovangrandi, Lab on a Chip, 2013 Feb. 21; 13(4):722-9. doi: 10.1039/c2lc40896a.

[0177] [22] Morgan E[1], Varro R, Sepulveda H, Ember J A, Apgar J, Wilson J, Lowe L, Chen R, Shivraj L, Agadir A, Campos R, Ernst D, Gaur A. *Clin Immunol.* 2004 March; 110(3):252-66.

[0178] [23] D. Holmes, D. Pettigrew, C. H. Reccius, J. D. Gwyer, C. van Berkel, J.

[0179] Holloway, D. E. Davies, and H. Morgan, *Lab on a Chip* 9. 2881 (2009).

[0180] [24] X. Han, C. van Berkel, J. Gwyer, L. Capretto, and H. Morgan, *Analytical Chemistry* 84, 1070 (2012).

What is claimed is:

1. A method of establishing a differential white blood cell count comprising:

directing at least one stream of deionized water into a microfluidic device containing a sample of whole blood

of a subject or a cell-rich fraction of a whole blood sample or a cell-free fraction of whole blood of a subject or combinations thereof to generate a lysate stream of intact white blood cells;

directing at least one stream of deionized water into the lysate stream such that the lysate stream with intact white blood cells is forced to flow in a direction of motion by the at least one stream of deionized water to form a virtual non-conductive aperture in a channel of the microfluidic device; and

performing impedance cytometry of the lysate stream in the virtual non-conductive aperture via coplanar electrodes to detect the presence of intact white blood cells in the lysate stream.

2. The method according to claim **1**, further comprising

quantitatively differentiating between neutrophils, lymphocytes, monocytes, eosinophils, and basophils in the lysate stream based on the impedance measurements resulting from the performance of the impedance cytometry.

3. The method according to claim **1**, wherein the step of directing at least ONE stream of deionized water into the channel includes symmetrically focusing at least two streams of deionized water orthogonally on opposing sides of the direction of motion of the lysate stream to form the virtual non-conductive aperture.

4. A method of fabricating a microfluidic device comprising:

forming a layer of material on a substrate and adhering a plurality of pairs of co-planar electrodes on the substrate; and

forming a plurality of microchannels in the layer of material,

wherein at least one of the microchannels is configured and disposed to receive at least one stream of deionized water to effect lysis of a whole blood sample or of a cell-rich fraction of a whole blood sample to produce a lysate stream,

wherein at least one of the microchannels is configured and disposed to receive the lysate stream and to receive at least one focusing flow of deionized water to effect a virtual aperture and

wherein at least one the pairs of co-planar electrodes is formed under one of the plurality of microchannels in which is generated the virtual aperture such that impedance cytometry of the lysate stream in the virtual aperture is enabled by application of an electric field to at least two pairs of the plurality of pairs of co-planar electrodes.

5. The method of fabricating according to claim **4**, wherein the step of adhering a plurality of pairs of co-planar electrodes on the substrate includes applying a chrome adhesive between the plurality of pairs of co-planar electrodes and the substrate.

6. A microfluidic device comprising:

a layer of material formed over a substrate;

a blood separation section configured and disposed in the layer of material to receive a sample of whole blood of a subject and to separate the whole blood sample into a cell-free fraction and into a cell-rich fraction;

an analyte sensor section configured and disposed in the layer of material to detect an analyte in the cell-free fraction via application of an electrical field and detection of changes in at least one electrical property in the analyte;

a cell pre-treatment section configured and disposed in the layer of material to form a lysate from the cell-rich fraction; and

a cell or large particle analyzer section configured and disposed on the layer of material to enable analysis of the lysate from the cell-rich fraction to detect circulating tumor cells or white blood cells including neutrophils, lymphocytes, monocytes, eosinophils, and basophils.

7. The microfluidic device according to claim **6**, wherein the cell or large particle analyzer section is configured and disposed on the layer of material to enable analysis of the lysate from the cell-rich fraction to enable a differential white blood cell count via coplanar electrodes formed over the substrate that are configured and disposed to enable impedance cytometry of the white blood cells in the cell or large particle analyzer section.

8. A microfluidic device for establishing a differential white blood cell count comprising:

a substrate:

a layer of material formed over the substrate: and

a plurality of microchannels formed in the layer of material,

at least one of the plurality of microchannels configured and disposed to receive a sample of whole blood of a subject or a cell-rich fraction of a whole blood or combinations thereof,

wherein at least one of the plurality of microchannels is configured and disposed to receive at least one stream of deionized water to effect lysis of a whole blood sample or of a cell-rich fraction of a whole blood sample to produce a lysate stream,

wherein at least one of the plurality of microchannels is configured and disposed to receive the lysate stream and to receive at least one focusing flow of deionized water to effect a virtual aperture and

wherein at least one the pairs of co-planar electrodes is formed under one of the plurality of microchannels in which is generated the virtual aperture such that impedance cytometry of the lysate stream in the virtual aperture is enabled by application of an electric field to at least two pairs of the plurality of pairs of co-planar electrodes.

9. The microfluidic device according to claim **8**, wherein with respect to the at least one of the plurality of microchannels that is configured and disposed to receive the lysate stream and to receive at least one focusing flow of deionized water to effect a virtual aperture,

the plurality of microchannels comprises at least two deionized water injection channels and a lysate stream channel such that the at least two deionized water injection channels are configured and disposed to symmetrically focus at least two streams of deionized water orthogonally on opposing sides of a direction of motion of the lysate stream in the lysate stream channel.

* * * * *